

**Experience-Dependent Dendrite Remodeling
of GABAergic Interneurons in the Adult Visual Cortex**

by

Jerry L. Chen

B.A., Molecular and Cellular Biology
University of California, Berkeley, 2003

Submitted to the Department of Biology in Partial
Fulfillment of the Requirements for the Degree of

Doctor of Philosophy in Biology

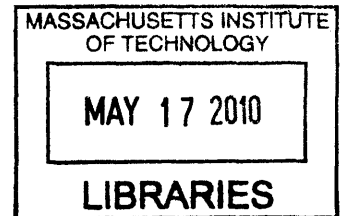
at the

Massachusetts Institute of Technology

June 2010

© 2010 Massachusetts Institute of Technology
All rights reserved

ARCHIVES



Signature of Author: _____

[Handwritten signature]

Department of Biology
June 3, 2010

Certified by: _____

[Handwritten signature]

Elly Nedivi
Associate Professor of Neurobiology
Thesis Supervisor

Accepted by: _____

[Handwritten signature]

Stephen P. Bell
Professor of Biology
Chairman, Committee for Graduate Students

Experience-Dependent Dendrite Remodeling of GABAergic Interneurons in the Adult Visual Cortex

by

Jerry L. Chen

Submitted to the Department of Biology
on May 21, 2010 in Partial Fulfillment of the
Requirements for the Degree of
Doctor of Philosophy in Biology

ABSTRACT

An ever increasing amount of evidence is demonstrating that structural plasticity is a diverse and ongoing feature that contributes to plasticity in the adult brain. It was previously shown that dendritic arbors of inhibitory interneurons in superficial layer 2/3 can remodel in the adult cortex. Here, we investigated the role of these structural rearrangements during experience-dependent adult plasticity. Using *in vivo* two photon imaging, we monitored interneuron dendritic branch tip remodeling in response to changes in visual experience in the adult mouse visual cortex. We find that branch tip dynamics are induced by novel experiences in a stimulus-specific manner. Visual deprivation produces rearrangements that are circuit-specific and are different for branch tips extending into L1 or L2/3. The weakening of dendritic input onto these cells functions to reduce levels of inhibition in local cortical circuits. This reduced inhibitory tone provides more salience to remaining instructive input, allowing more structural and functional adaptations to occur.

In order to better understand how synaptic plasticity accompanies these dendritic arbor rearrangements as well as other forms of structural plasticity, we developed a method to simultaneously monitor structural and synaptic dynamics in the mammalian brain using *in vivo* two-photon microscopy. Structural and synaptic components can be labeled in cortical neurons of mice in a cell type and laminar specific manner through co-injection of independent lentiviral vectors at a late embryonic or early postnatal age. We demonstrate that excitatory and inhibitory post-synaptic densities can be visualized by tagging fluorescent proteins to PSD95 and Gephyrin, respectively. Finally, we show that the fluorescent proteins, Teal and Venus, can be simultaneously excited and spectrally resolved through linear unmixing so that individual structural and synaptic components can be identified and followed over time. Through this approach, the relationship between synaptic and structural plasticity can be studied in the living brain.

Thesis Supervisor: Elly Nedivi
Title: Associate Professor of Neurobiology

Acknowledgements

I would first like to thank my advisor, Elly Nedivi, for all her support and for everything she has taught about being a scientist. Looking back, her influence on me has been immeasurable.

I would like to thank my committee: Matthew Wilson, Joshua Sanes, and especially Martha Constantine-Paton and Carlos Lois for their helpful input along the way.

I would also like to thank Wei-Chung Allen Lee for helping get me started in the lab as well as all of the members of the Nedivi lab who have helped along the way: Corey, Zhen, Tad, Putz, Jo, Sven, Jen, Alan, Mike, Rachel, Gen, Monica, Walter, Ronen, Amy, Charles. This includes the undergraduate students that I've had the pleasure to work with: Christopher, Isabelle, Mariel, Sonia.

Furthermore, I would like to thank my collaborators: Jaewon Cha, Heejin Choi, and Peter So for making my experiments run and for bringing out a little of the engineer in me, as well as Jason Coleman and Yasunobu Murata for their ongoing exchange of ideas, reagents, and equipment.

Finally, I would like to thank my parents for everything they have done and will ever do, and Ines for helping to see me through all the way.

Table of Contents

Chapter 1: Introduction	5
Structural Plasticity in the Adult Cortex	6
Ocular Dominance Plasticity	10
GABA-Mediated Inhibition in Adult Cortical Plasticity	11
<i>In Vivo</i> Two-Photon Microscopy	13
Summary	14
Chapter 2: Structural Basis for the Role of Inhibition in Facilitating Adult Brain Plasticity	16
Abstract	16
Introduction	17
Results	18
Discussion	26
Methods	35
Figures	40
Supplemental Data	47
Chapter 3: Towards Dual Color Imaging of Structural and Synaptic Plasticity <i>In Vivo</i>	50
Abstract	50
Introduction	51
Results	52
Discussion	58
Methods	63
Figures	69
Tables	77
Chapter 4: Conclusion	78
Structural and Inhibitory-Mediated Plasticity in the Adult Cortex	78
Novel and Learned Experiences in the Adult Cortex	81
Future Experiments	83
References	86

CHAPTER 1

Introduction

Plasticity is a fundamental feature of the brain that is critical throughout the life of an animal as it makes its way through its environment. Exactly how and where plasticity occurs in the brain is an ongoing question in neuroscience. In the mammalian system, the cerebral cortex is a region thought to underlie learning, memory, perception, attention, and consciousness. Ever since the first descriptions of the anatomy and morphology of individual cortical neurons (Ramón y Cajal 1911), it has been clear that the anatomical organization of the cortex contributes to its function.

Cortical circuits are built upon a laminar architecture consisting of excitatory pyramidal neurons and inhibitory interneurons of various cell types (Douglas and Martin 2004). Neurons transmit activity locally or over long distances through axonal arbors containing boutons which form synapses at various sites on the post-synaptic cell. A large fraction of excitatory synapses are made on dendritic spines that protrude from the dendrites of pyramidal neurons (Peters 2002). For aspiny interneurons, excitatory synapses are largely made on dendritic shafts (Markram, Toledo-Rodriguez et al. 2004). Axons of inhibitory neurons form dendritic shaft synapses as well as perisomatic and axo-axonic synapses (Somogyi, Tamas et al. 1998).

In order to alter the way cortical circuits process neuronal activity in response to changes in experience, neuronal plasticity has been shown to take many forms, from

changes in intrinsic excitability, to alterations in the strength of existing synapses, to structural changes that result in the formation or elimination of synaptic connections (Feldman 2009). The long-term nature of structural changes make them attractive as cellular substrates for persistent changes in connectivity, such as might be required for learning and memory (Bailey and Kandel 1993) or changes in cortical map representation (Buonomano and Merzenich 1998).

During development, structural plasticity is needed for the formation and maturation of cortical circuits, initially driven by intrinsic genetic programs and spontaneous activity and later increasingly sensitive to activity driven by sensory experience (Katz and Shatz 1996). As an animal fully matures and a developmental critical period comes to an end (Hensch 2005), the cortex exhibits a reduced capacity to adapt both functionally and structurally in response to changes in experience.

STRUCTURAL PLASTICITY IN THE ADULT CORTEX

The degree to which structural plasticity occurs in the adult brain and to what extent it may contribute to experience-dependent modifications of functional circuitry has been a long debated question in neuroscience. Historically, structural rearrangements in the adult brain have largely been measured in post-mortem tissue in which large-scale axonal remodeling in response to injury-related perturbations have been shown to occur (Darian-Smith and Gilbert 1994; Florence, Taub et al. 1998). The nature of these studies are only revealing of large scale, net changes occurring with little information about the dynamics and the full range of modifications that could be

taking place on a day-to-day basis. The development of techniques for stable neuronal labeling (Feng, Mellor et al. 2000; Dittgen, Nimmerjahn et al. 2004) and implementation of two-photon microscopy for imaging deep into scattering tissue (Denk, Strickler et al. 1990) have enabled for the first time longitudinal observations of structural dynamics in cerebral cortical neurons embedded within an intact circuit.

While limits in optical penetration has largely confined *in vivo* two photon imaging to structures extending into L1 and L2/3, it seems clear that a fraction of neuronal structures are highly dynamic and responsive to experience. Day-to-day axonal arbor and bouton dynamics have been shown to occur in the adult cortex. L6 pyramidal and thalamocortical axons innervating L1 and L2/3 can remodel up to $\sim 30\mu\text{m}$ over 4 days (De Paola, Holtmaat et al. 2006). While L6 pyramidal neurons contain more dynamic *terminaux* boutons (TBs) with a turnover rate of $\sim 20\%$ per week, thalamocortical axons contain a mixture of *en passant* boutons (EPBs) and TBs which turnover around $\sim 4\%$ and $\sim 7\%$ per week, respectively. This bouton turnover is not necessarily indicative of one-to-one synaptic gain or loss as boutons can vary in their number of synaptic connections from a few to even none (White, Weinfeld et al. 2004), and both excitatory and inhibitory boutons can partner with the same dendritic spine (Jones and Powell 1969). Horizontal projections of L2/3 pyramidal neurons contain a high density of EPBs, approximately 7-12% of which turnover per week under normal experience but whose arbors appear stable (Stettler, Yamahachi et al. 2006). However, a focal retinal lesion can produce a 5-10 fold increase in axonal bouton turnover in these cells (Yamahachi, Marik et al. 2009), accompanied by rapid initial growth of axonal arbors on the order of tens of microns from surrounding horizontal projections into the deprived region followed by a steady period of retractions over the course of weeks.

A considerable amount of attention has been focused on the structural dynamics of dendritic spines, as they are thought to provide a one-to-one indicator of excitatory synaptic presence (Grutzendler, Kasthuri et al. 2002; Trachtenberg, Chen et al. 2002; Holtmaat, Trachtenberg et al. 2005; Holtmaat, Wilbrecht et al. 2006; Majewska, Newton et al. 2006; Keck, Mrsic-Flogel et al. 2008; Hofer, Mrsic-Flogel et al. 2009; Xu, Yu et al. 2009; Yang, Pan et al. 2009). In reality, the one-to-one correspondence between dendritic spine and excitatory synapse are less straightforward. For example, evidence shows that about 2-4% spines in the neocortex lack synapses (White and Rock 1980; Hersch and White 1981; Benshalom and White 1986; Arellano, Espinosa et al. 2007). New spines can require a period of up to 4 days to form a synapse and can form synapses with boutons containing multiple synaptic partners (Knott, Holtmaat et al. 2006). Despite these reservations, dendritic spine dynamics give us the closest estimation of excitatory on excitatory synaptic dynamics without visualizing synapses directly. It appears that approximately ~5-10% of spines on layer 5 (L5) apical dendrites and L2/3 pyramidal neurons can form or be eliminated over the course of a week in response to normal, day-to-day experience. This degree of spine dynamics can vary across different primary sensory areas suggesting that the requirement for structural plasticity may differ by cortical region.

Sensory manipulations leading to alterations in cortical representation such as chessboard whisker trimming, monocular deprivation, or retinal lesion can produce up to a three-fold increase in the rate of spine turnover (Trachtenberg, Chen et al. 2002; Holtmaat, Wilbrecht et al. 2006; Keck, Mrsic-Flogel et al. 2008; Hofer, Mrsic-Flogel et al. 2009). More recently, behavioral learning through motor training has been shown to produce increases in spine dynamics of up to 10% in the adult motor cortex, comparable

to that of sensory deprivation (Xu, Yu et al. 2009; Yang, Pan et al. 2009). In the case of a retinal lesion, the observed increased spine turnover is accompanied by an almost complete replacement of 90% of the initial spines in the silenced region of visual cortex during retinotopic reorganization (Keck, Mrsic-Flogel et al. 2008).

Aside from dendritic spines, the dendritic arbors of pyramidal neurons are largely stable in the adult cortex (Trachtenberg, Chen et al. 2002; Lee, Huang et al. 2006), although some mouse mutants show uncharacteristically large dendritic remodeling. For example, delta-catenin knock out animals show a progressive loss of dendrites and spines concomitant with a decrease in cortical function (Matter, Pribadi et al. 2009). In mice with a late onset deletion of the Pten tumor suppressor gene, apical dendrites of L2/3 pyramidal neurons continued to grow and expand in the mature cortex, while basal dendrites within the same neuron or apical dendrites of L5 pyramidal neurons were unaffected (Chow, Groszer et al. 2009). These studies reveal a latent capacity for large scale dendrite remodeling in the adult cortex.

Unlike pyramidal neurons, ~3% of dendritic branch tips on inhibitory interneurons can remodel on a day-to-day basis. Each dynamic branch tip can elongate or retract between 5-20 μm per week with total changes of to up $\sim 80\mu\text{m}$ over weeks (Lee, Huang et al. 2006). These remodeling interneurons are not subtype specific but reside within a superficial strip of L2/3 (Lee, Chen et al. 2008). Since only a minority of inhibitory cells contain spines, the localization and hence plasticity of excitatory synapses on these cells is less obvious. Serial EM reconstructions of interneuron dendrites indicate they contain a synaptic density of about one synapse per micron, ~80% of which are excitatory (Kubota, Karube et al. 2007). Thus, a significant degree

of synaptic reorganization is likely to accompany dendritic rearrangements on inhibitory neurons.

OCULAR DOMINANCE PLASTICITY

Ocular dominance (OD) plasticity in the visual system has been one of the more widely used model systems for studying the mechanisms of cortical plasticity. It was discovered that the binocular representation in primary visual cortex can be altered when one eye is closed for a period of time, leading to a decreased cortical response to the deprived eye and an increased response to the non-deprived eye (Wiesel and Hubel 1963). This form of plasticity has been observed in several mammalian species when induced by monocular deprivation (MD) (Wiesel and Hubel 1965; Hubel, Wiesel et al. 1977; Drager 1978) and appears to be either restricted to or particularly sensitive during the developmental critical period (Hubel and Wiesel 1970; Gordon and Stryker 1996). During this period, structural changes have been shown to accompany this functional plasticity (Hubel, Wiesel et al. 1977; Shatz and Stryker 1978; Antonini, Fagiolini et al. 1999). In particular, thalamocortical projections into primary visual cortex from the lateral geniculate nucleus of the non-deprived eye have been shown to take over cortical space at the expense of deprived eye projections, providing evidence that structural plasticity participates in OD plasticity.

In recent years, more extensive studies of OD plasticity in the mouse visual system have led to the proposal of several mechanisms explaining this phenomenon in cortex from long-term potentiation/depression-like mechanisms (Smith, Heynen et al.

2009) to homeostatic synaptic plasticity (Turrigiano and Nelson 2004) to regulation by inhibitory circuits (Hensch 2005). These proposed mechanisms at times seem at odds with one another, thus complicating our understanding of OD plasticity. Adding to this complication is the discovery that unlike in cat, ferret, or monkey, OD plasticity in the mouse can extend into adulthood (Sawtell, Frenkel et al. 2003; Frenkel, Sawtell et al. 2006; Hofer, Mrsic-Flogel et al. 2006; Sato and Stryker 2008). Other than a clear requirement for a prolonged period of MD to produce an OD shift in the adult, the mechanistic differences in OD plasticity during development and adulthood remain largely unknown. While extensive structural remodeling has yet to be observed during adult OD plasticity, finer scale changes such as the formation of dendritic spines have been shown to occur (Hofer, Mrsic-Flogel et al. 2009). Emerging studies have also indicated that OD plasticity differs between excitatory pyramidal neurons and inhibitory interneurons during development and that these differences evolve as the animal matures into adulthood (Gandhi, Yanagawa et al. 2008; Yazaki-Sugiyama, Kang et al. 2009; Kameyama, Sohya et al. 2010).

GABA-MEDIATED INHIBITION IN ADULT CORTICAL PLASTICITY

Inhibitory interneurons, which use γ -aminobutyric acid (GABA) as their neurotransmitter, represent approximately 20% of the neuronal population in the cortex and are highly diverse in their morphology, electrophysiological properties, molecular expression, and axonal targeting (Markram, Toledo-Rodriguez et al. 2004). They have been shown to function locally in modulating the gain and synchrony of activity in

cortical circuits of excitatory neurons (Singer 1996; McBain and Fisahn 2001). Cortical interneurons are also thought to shape receptive fields as well as to generate cortical oscillations and set network states (Alitto and Dan 2010). During development, the maturation of GABAergic interneurons and the accompanying increase in intracortical inhibition has been shown to trigger the onset (Fagiolini and Hensch 2000) and closure (Hanover, Huang et al. 1999; Huang, Kirkwood et al. 1999) of critical period OD plasticity. These findings suggest that the inhibitory tone established at the end of the critical period restricts the levels or patterns of activity that may be required to produce cortical plasticity.

In the adult, changes in visual experience can still alter levels of GABAergic inhibition. Loss of visual input in one eye through lid suture, enucleation, or tetrodotoxin injection resulted in a decreased expression in GABA, GABA receptor, and the GABA synthesizing enzyme, glutamate decarboxylase, specifically in the deprived-eye column in monkey visual cortex (Hendry and Jones 1986; Hendry and Jones 1988; Hendry, Fuchs et al. 1990; Hendry, Huntsman et al. 1994). In rats, this reduction in intracortical inhibition has been associated with the restoration of a juvenile form of plasticity in adult cortex. Direct blockade of GABAergic inhibition in visual cortex reactivates OD plasticity in response to MD in adult rats (Harauzov, Spolidoro et al. 2010). Reduced intracortical inhibition and restored cortical plasticity can also be achieved in an experience-dependent manner. A period of visual deprivation by dark rearing in adult rats can result in a juvenile form of OD plasticity upon MD as well a reduction in GABA_A receptors (He, Hodos et al. 2006). Environmental enrichment has also been shown to lead to a reduction in inhibitory tone in the adult rat as well as promoting a full recovery from a normally irreversible OD shift induced during a

juvenile MD (Sale, Maya Vetencourt et al. 2007). Similar effects have also been achieved with pharmacological treatment of the selective serotonin reuptake inhibitor, fluoxetine, which also produces a reduction in inhibition and a juvenile state of plasticity in the adult (Maya Vetencourt, Sale et al. 2008). These studies suggest GABAergic inhibition can be modulated by experience and regulate the capacity for plasticity in the adult cortex.

***IN VIVO* TWO-PHOTON MICROSCOPY**

The initial proposal of fluorescence excitation by two-photon absorption in the early 1930s (Göppert-Mayer 1931) followed by its later implementation in living cells at the end of the century (Denk, Strickler et al. 1990) has ushered in a range of new applications for the field of neurosciences. *In vivo* two-photon microscopy has already been applied to observe the dynamics of neuronal morphology and activity as well as disease states in the brain (Helmchen and Denk 2005). Two-photon excitation occurs when two photons arrive simultaneously, combining their energies, to drive a molecule to an excited state whereby an emission photon will be produced. This nonlinear process in two-photon microscopy offers several advantages compared to traditional forms of light microscopy. First, since the light source for two-photon excitation is generally, approximately half the energy of single photon excitation, conventional fluorophores which typically emit in the visible spectrum require an excitation in the near-infrared wavelength range. This excitation wavelength can penetrate deeper into scattering tissue and is generally less phototoxic compared to ‘bluer’ light. Second,

since the probability of achieving two-photon excitation depends supralinearly on the density of photons, two-photon excitation is restricted to a sub-micron volume at the focal point. This feature reduces photo-damage and provides three-dimensional optical sectioning of tissue.

The parallel development of *in vivo* fluorescence labeling techniques has allowed the potential of two-photon microscopy to come to full fruition. Genetically encoded fluorophores are used throughout research in biology today (Shaner, Steinbach et al. 2005; Day and Davidson 2009). For their use in *in vivo* two-photon imaging, fluorescent proteins must be photostable and bright enough to yield sufficient signal for reliable detectability. They must also express efficiently, without toxicity, and should not oligomerize if used as a fusion protein to tag molecules of interest. Up to this point, green or yellow fluorescent protein, expressed cytoplasmically, have typically been used to label and image neuronal structures in the brain. Stable, single cell labeling has been achieved through the generation of transgenic animals (Feng, Mellor et al. 2000) or through viral-mediated gene delivery (Dittgen, Nimmerjahn et al. 2004). This has been the predominant mode for carrying out *in vivo* studies of structural plasticity in the mammalian brain (Holtmaat and Svoboda 2009).

SUMMARY

While it is becoming evident that structural plasticity occurs in the adult cortex, its role in cortical plasticity remains unclear. Based upon our previous observation that dendritic arbors of superficial L2/3 interneurons remodel in the adult cortex, we

investigated the role of these structural rearrangements during experience-dependent adult plasticity. Using *in vivo* two photon imaging, we monitored interneuron dendritic branch tip remodeling during OD plasticity in the adult mouse visual cortex. We asked whether changes in visual experience can drive branch tip dynamics in a stimulus- and circuit-specific manner. We also asked whether these changes can contribute to altered levels of intracortical inhibition that serves to mediate plasticity in the adult cortex.

In order to better understand how synaptic plasticity accompanies these dendritic arbor rearrangements as well as other forms of structural plasticity, we sought to develop a method to simultaneously monitor structural and synaptic dynamics in the mammalian brain using *in vivo* two-photon microscopy. To this end, we determined whether excitatory and inhibitory synaptic components could be sufficiently labeled for reliable visualization across time. We explored methods to achieve dual gene expression of structural and synaptic labeling in neurons in a cell-type and laminar specific manner. We also sought to identify combinations of fluorescent proteins that can be simultaneously excited and spectrally resolved during *in vivo* two-photon imaging. The application of such a technique would aid in assessing the relationship between structural and synaptic plasticity in the adult brain.

CHAPTER 2

Structural Basis for the Role of Inhibition in Facilitating Adult Brain Plasticity

Experiments presented in Figure 6 were carried out in collaboration with Walter C. Lin

ABSTRACT

While inhibition has been implicated in mediating plasticity in the adult brain, the mechanism remains unclear. Here we present a structural mechanism for the role of inhibition in experience-dependent plasticity. Using chronic *in vivo* two-photon microscopy we show that experience drives structural remodeling of superficial cortical layer 2/3 interneurons in an input- and circuit-specific manner, with up to 15% of branch tips remodeling. Visual deprivation induces different branch tip dynamics in dendrites extending into layer 1 versus layer 2/3. This produces an initial weakening of feedforward input onto supragranular interneurons. The resulting decrease in inhibitory tone, also achievable pharmacologically by the antidepressant fluoxetine, provides a permissive environment for further structural and functional adaptation. Our findings suggest that therapeutic approaches that reduce inhibition, when combined with an instructive stimulus, could serve to structurally modify mature circuits impaired by neurological damage or disease, improving function and perhaps enhancing cognitive abilities.

INTRODUCTION

Promoting plasticity, the ability to adapt, in the adult brain is critically important for enabling functional recovery from disease or injury related neurological damage and for enhancing cognitive abilities such as learning and memory. It is increasingly evident that inhibitory circuits play a key role in neurological deficits as well as experience-dependent plasticity. A variety of genetic disorders that present cognitive deficits, such as autism, Rett and Down syndromes have been associated with excessive inhibition (Rubenstein and Merzenich 2003; Kleschevnikov, Belichenko et al. 2004; Dani, Chang et al. 2005). In the case of Down syndrome, reducing inhibition can improve cognitive function (Fernandez, Morishita et al. 2007). Reducing intracortical inhibition in the visual system, either pharmacologically, through sensory deprivation, or by environmental enrichment has been shown to restore a juvenile state of plasticity in the adult brain (He, Hodos et al. 2006; Sale, Maya Vetencourt et al. 2007; Maya Vetencourt, Sale et al. 2008). Thus, modification of inhibitory circuits could provide an important therapeutic approach. Yet, the mechanism whereby experience alters inhibitory circuitry is unclear, and the extent to which these circuits can be modified in a spatially restricted manner remains unaddressed.

Using a multi-photon microscope system for chronic *in vivo* imaging of neuronal morphology in the intact rodent cerebral cortex, we previously showed that dendrites of inhibitory interneurons in the adult visual cortex remodel on a day-to-day basis (Lee, Huang et al. 2006). These remodeling interneurons are not subtype specific but reside within a "dynamic zone" corresponding to a superficial strip of layer 2/3 (L2/3) (Lee, Chen et al. 2008). Electrophysiological studies suggest that the supragranular layers of

cortex retain a unique capacity for plasticity that persists beyond development into adulthood (LeVay, Wiesel et al. 1980; Daw, Fox et al. 1992; Hirsch and Gilbert 1993). We hypothesized that the structural rearrangement of dynamic zone interneurons provides a mechanism for experience-dependent functional plasticity in the adult cortex. To test this hypothesis we monitored entire dendritic arbors of superficial L2/3 interneurons in the visual cortex of adult mice subjected to monocular deprivation (MD) or binocular deprivation (BD), classic paradigms for investigating experience-dependent plasticity in the visual system.

RESULTS

MD Increases Branch Tip Dynamics in Binocular but not Monocular Visual

Cortex

Adult thy1-GFP-S transgenic mice (postnatal day 42–56) expressing GFP in a random subset of neurons sparsely distributed within the superficial cortical layers were surgically implanted with bilateral cranial windows over the visual cortices. Following 3 weeks of recovery, superficial L2/3 interneurons (65-150 μ m below the pial surface) were identified and a two-photon imaging volume encompassing the cell and all of its dendritic arbors was acquired. Cells were imaged weekly while the animal experienced an initial two-week period of normal vision followed by a 14-day MD of the contralateral eye or a 14-day BD, with an intermediate imaging session performed after 4 days of deprivation (Figure 1A). To ascertain the location of each cell soma with respect to binocular and monocular visual cortex, optical intrinsic signal imaging was

performed after the first two-photon imaging session (Figure 1B, see also Figure S1). In addition, at the conclusion of the two-photon imaging time course, a transneuronal tracer, wheat germ agglutinin-Alexa555 (WGA-555), was injected into the ipsilateral eye. The coronal section containing the imaged cell in the fixed brain was identified to confirm cell depth and location within visual cortex through a combination of DAPI staining, revealing cortical laminae, and WGA-555 labeling of thalamocortical projections from the ipsilateral eye, revealing binocular visual cortex (Figure 1C).

Ocular dominance (OD) plasticity induced by MD in the adult mouse is characterized by a clear potentiation of the non-deprived ipsilateral eye response and by a slight depression of the deprived contralateral eye response (Sawtell, Frenkel et al. 2003; Frenkel, Sawtell et al. 2006; Hofer, Mrsic-Flogel et al. 2006; Sato and Stryker 2008; Hofer, Mrsic-Flogel et al. 2009) specific to binocular visual cortex. More recently, L2/3 interneurons in binocular visual cortex were shown to exhibit an even stronger OD shift in response to MD than pyramidal cells largely due to a more robust depression of the deprived eye response (Kameyama, Sohya et al. 2010). Chronic two-photon imaging of superficial L2/3 interneurons in binocular visual cortex revealed that under normal vision, $2.98 \pm 0.48\%$ (mean \pm s.e.m.) of monitored dendritic branch tips remodel per week with $14.8 \pm 1.8\%$ of all branch tips remodeling during the entire time course (Figure 1D, 2A, C). Each branch tip length change was an average of $8.65 \pm 1.40 \mu\text{m}$ per week or up to $45 \mu\text{m}$ over the entire time course and included elongations and retractions of existing branch tips as well as the formation and elimination of entire branch tips (Figure 1D-F). MD led to a 3-fold increase in branch tip dynamics compared to normal vision to $9.02 \pm 2.01\%$ at 0-4d MD, and $8.52 \pm 1.70\%$ at 4-7d MD (control versus 0-4d MD, Wilcoxon rank sum test, $p < 0.005$; control versus 4-7d MD,

Wilcoxon rank sum test, $p < 0.01$). This increase in dynamics consisted of a total branch tip length change of $32.7 \pm 5.7 \mu\text{m}$ per cell or $1.81 \pm 0.31\%$ of the total branch tip length per cell (Figure 2D). However, the average length change per branch tip did not increase (Mann-Whitney U -test, $p = 0.96$) suggesting that the primary effect of MD on branch tip rearrangements is to increase the number of dynamic branch tips. The 7 days of increased branch tip dynamics after MD coincides with the time required for a functional OD shift to occur in the adult mouse (Sawtell, Frenkel et al. 2003; Frenkel, Sawtell et al. 2006; Hofer, Mrsic-Flogel et al. 2006; Sato and Stryker 2008; Hofer, Mrsic-Flogel et al. 2009). MD beyond 7 days does not elicit a further OD shift (Sato and Stryker 2008). Correspondingly, we found that branch tip dynamics decreased below baseline levels from 7-14 d MD (control versus 7-14d MD, Wilcoxon rank sum test, $p < 0.05$). This demonstrates that interneuron dendritic branch tip rearrangement is enhanced during OD plasticity in binocular visual cortex.

In monocular visual cortex, branch tip dynamics during normal vision in superficial L2/3 interneurons was $3.15 \pm 0.61\%$ per week, comparable to that in binocular visual cortex (Figure 2B and C). MD led to an initial decrease in branch tip dynamics from 0-4d MD (control versus 0-4d MD, Wilcoxon rank sum test, $p < 0.05$). However, branch tip dynamics returned to baseline rates from 4-7d MD and 7-14d MD (control versus 4-7d MD, Wilcoxon rank sum test, $p = 0.39$; control versus 7-14d MD, Wilcoxon rank sum test, $p = 0.07$). The initial decrease in branch tip dynamics likely reflects the loss of visual drive to monocular visual cortex, while the recovery to baseline levels between 4-7d MD and 7-14d MD may reflect the restoration of cortical activity brought about by homeostatic mechanisms such as synaptic scaling or increased

intrinsic excitability, as previously observed after sensory deprivation (Goel and Lee 2007; Maffei and Turrigiano 2008).

Recovery and Repeated MD does not Increase Branch Tip Dynamics in Binocular Visual Cortex

It is thought that structural rearrangements are primarily induced by novel experiences and can persist beyond the initial experience to facilitate functional responses to repeated experience (Hofer, Mrsic-Flogel et al. 2009; Xu, Yu et al. 2009; Yang, Pan et al. 2009). Re-opening of the deprived eye after a prolonged MD leads to recovery in OD after at least 7 days of normal vision (Hofer, Mrsic-Flogel et al. 2006) but is not accompanied by increased dendritic spine dynamics (Hofer, Mrsic-Flogel et al. 2009). To determine if branch tip rearrangements accompanies functional recovery, we imaged interneuron branch tip remodeling for 3 weeks following a 14-day MD (Figure 3A and B). Branch tip dynamics was not increased compared to control (control versus recovery, Mann-Whitney U -test, $p = 0.82$) suggesting that functional recovery from MD does not involve interneuron branch tip remodelling. A second brief MD following recovery can produce an immediate OD shift (Hofer, Mrsic-Flogel et al. 2006). Unlike during an initial MD, a second MD was not accompanied by an increase in dendritic spine dynamics (Hofer, Mrsic-Flogel et al. 2009). Similarly, we found that a brief 3-day second MD performed after 3 weeks of recovery did not increase interneuron branch tip dynamics (control versus second MD, Mann-Whitney U -test, $p = 0.54$) suggesting that OD shifts from a repeated MD does not involve interneuron branch tip remodeling.

Experience Induced Branch Tip Rearrangements are Stimulus and Laminar-Specific

Superficial L2/3 has been identified as a region where bottom-up feedforward inputs carrying basic sensory information (Nassi and Callaway 2009) converge with top-down feedback inputs modulating attention, response strength, and saliency (Rockland and Pandya 1979; Maunsell and van Essen 1983; Bullier, Hupe et al. 2001) in the non-human primate visual system. The laminar restriction of interneuron dendritic remodeling to superficial L2/3 (Lee, Chen et al. 2008) and the presence of these anatomical pathways in the mouse visual cortex (Antonini, Fagiolini et al. 1999; Yamashita, Valkova et al. 2003; Dong, Shao et al. 2004; Dong, Wang et al. 2004) led us to propose that inhibitory circuit restructuring specifically in this locale serves to coordinate the relative contribution of these two pathways to visual processing. To test this hypothesis, we explored whether MD, which directly and selectively alters the feedforward pathway, affects branch tip dynamics in a spatially-restricted manner that reflects pathway-specific rewiring. We examined the position of dynamic branch tips before and during the first 7 days of MD in binocular visual cortex with respect to laminar location (Figure 4A). Under normal vision, branch tip elongations were distributed with 63% in L1 (0-65 μ m below the pial surface), an area dominated by feedback input, and 37% in superficial L2/3 (65-150 μ m), a location more strongly influenced by feedforward thalamic input (Figure 4B). Branch tip retractions were distributed with 54% in L1 and 46% in superficial L2/3. At 0-4d MD, this distribution changes dramatically such that 88% of branch tip retractions occur within L2/3 (control retraction versus 0-4d MD retractions, K-S test, $p < 0.05$). Closer analysis of branch tip dynamics by layer shows that in L2/3, MD led to an initial increase in branch tip

retractions from 0-4d MD followed by an increase in elongations from 4-7d MD (Figure 3C; Wilcoxon rank sum test, control versus 0-4d MD elongations, $p < 0.01$; Wilcoxon rank sum test, control versus 4-7d MD elongations: $p < 0.05$). In L1, only a brief increase in retractions was observed at 4-7d MD (control versus 4-7d MD retractions, Wilcoxon rank sum test, $p < 0.05$). By comparison, elongations and retractions remain balanced in L2/3 of monocular visual cortex during MD (Figure S2, 0-4d MD elongations versus retractions Wilcoxon rank sum test, $p = 0.69$; 4-7d MD elongations versus retractions Wilcoxon rank sum test, $p = 0.24$). These results demonstrate that in response to experience, superficial L2/3 interneurons of binocular visual cortex are capable of selectively re-distributing branch tips that are potentially receiving different inputs, visually-driven feedforward inputs in L2/3 or top-down inputs in L1.

Binocular deprivation as a visual manipulation distinct from MD has proven insightful in distinguishing between the role of sensory deprivation and sensory experience during experience-dependent plasticity (Wiesel and Hubel 1965; Gordon and Stryker 1996; Frenkel and Bear 2004; Sato and Stryker 2008). To determine the experience-dependent features of interneuron dendritic remodeling in binocular visual cortex, we compared MD-induced branch tips dynamics to those in animals subjected to a 14 day BD. Overall, BD in binocular visual cortex did not significantly increase the rate of branch tip remodeling in superficial L2/3 interneurons (Figure 5A, repeated measures ANOVA, $p = 0.28$). However, analysis by layer shows reduced elongations from 0-4d BD and reduced retractions from 4-7d BD for branch tips in L1 (Figure 5B, control versus 0-4d BD elongations, Wilcoxon rank sum test, $p < 0.05$; control versus 4-7d BD retractions, Wilcoxon rank sum test, $p < 0.05$). For branch tips in L2/3, BD led to an increase in retractions from 0-4d similar to that observed from 0-4d MD (control

versus 0-4d BD retractions, Wilcoxon rank sum test, $p < 0.05$). In contrast to increased branch tip elongations seen in this layer between 4-7d of MD, we observed further retractions between 4-7d of BD (control versus 4-7d BD retractions, Wilcoxon rank sum test, $p < 0.02$). These findings support the idea that branch tip remodeling in L2/3 specifically reflects changes in sensory input and that retractions observed in L2/3 during MD and BD in binocular visual cortex represent a deprivation-induced response. While monocular visual cortex during MD and binocular visual cortex during BD both experience a complete loss of visual activity, the lack of increased L2/3 retractions in monocular visual cortex during MD, suggests that the ipsilateral eye pathway is required for the retractions seen in binocular visual cortex between 0-4d MD. Furthermore, it suggests that the elongations in L2/3 of binocular visual cortex from 4-7d MD require sensory experience from the non-deprived eye.

Fluoxetine Mimics the Initial Effect of Sensory Deprivation in Facilitating Branch Tip Remodeling in Response to MD

Since approximately 80% of the synapses on interneuron dendrites are excitatory (Kubota, Karube et al. 2007), the primary effect of branch tip retractions elicited by sensory deprivation would likely be loss of excitatory input, resulting in reduced inhibition within the local circuit. It was previously shown that the widely used antidepressant drug, fluoxetine, can reduce intracortical inhibition and restore a juvenile form of OD plasticity in the adult rodent visual cortex (Maya Vetencourt, Sale et al. 2008). To further examine the role of intracortical inhibition in promoting visual cortical plasticity in the adult, we measured interneuron branch tip dynamics in binocular visual cortex in animals chronically administered fluoxetine for a period of

three weeks at a dosage previously shown to reduce cortical extracellular GABA. We then performed a brief 4d MD sufficient to induce a juvenile-like OD shift (Gordon and Stryker 1996; Frenkel and Bear 2004) while the animals continued to receive fluoxetine (Figure 6A). Under normal visual experience, fluoxetine treatment led to an increase in overall branch tip dynamics compared to control conditions (Figure 6B and C; control versus fluoxetine, Wilcoxon rank sum test, $p < 0.02$). These increased dynamics applied to both elongations and retractions in L1 as well as L2/3 (Figure 6C and S3A), suggesting that pharmacological reduction of intracortical inhibition by fluoxetine can promote structural remodeling in the adult brain. Interestingly, similarly to visual perturbations such as MD and BD, fluoxetine promotes remodeling of existing branch tips as opposed to the addition or elimination of entire branch tips (Figure S3B, C), suggesting that visual deprivations and fluoxetine may act through a common mechanism. Fluoxetine in combination with a brief 4d MD led to an immediate increase in elongations in L2/3 (Figure 6D, elongations versus retractions, Wilcoxon rank sum test, $p < 0.05$; fluoxetine versus 0-4d MD with fluoxetine, Wilcoxon rank sum test, $p < 0.05$). These increased elongations were similar to those observed during 4-7d MD without fluoxetine (0-4d MD versus 0-4d MD with fluoxetine, Mann-Whitney *U*-test, $p < 0.01$; 4-7d MD versus 0-4d MD with fluoxetine, Mann-Whitney *U*-test, $p = 0.62$). The accelerated time line of L2/3 remodeling seen with fluoxetine treatment, suggests that reduction of intracortical inhibition by fluoxetine can replace the initial period of deprivation-induced disinhibition in enabling further structural remodeling to occur.

DISCUSSION

While inhibition has been implicated in mediating plasticity in the adult brain (He, Hodos et al. 2006; Froemke, Merzenich et al. 2007; Sale, Maya Vetencourt et al. 2007; Maya Vetencourt, Sale et al. 2008), the mechanism has been unclear. Our findings suggest that structural remodeling of superficial L2/3 interneurons in an input-specific manner can sculpt mature inhibitory circuits so as to facilitate or attenuate experience-dependent plasticity.

Deprivation-Induced Dendritic Branch Tip Retractions in Interneurons

It is becoming increasingly apparent that MD induced OD plasticity produces different responses in inhibitory neurons as compared to excitatory neurons. During development, L2/3 inhibitory neurons exhibit a delayed OD plasticity compared to excitatory neurons in the same layer (Gandhi, Yanagawa et al. 2008). More recently, L2/3 fast-spiking interneurons have also been shown to exhibit a bidirectional plasticity during MD, initially shifting their preference to the deprived eye then shifting again to the non-deprived eye (Yazaki-Sugiyama, Kang et al. 2009). Differences between OD plasticity in excitatory and inhibitory neurons persist into adulthood. OD plasticity in excitatory neurons lacks the strong depression of the deprived eye response, and is mostly comprised of potentiation of the non-deprived eye response (Kameyama, Sohya et al. 2010). This is accompanied by an increase rather than loss of dendritic spines on excitatory cells, representing gain of excitatory synapses (Hofer, Mrsic-Flogel et al. 2009). We find that MD triggers an initial increase in L2/3 interneuron branch retractions concomitant with the strong depression of deprived eye response reported in these interneurons.

We find the increased L2/3 branch tip retractions in interneurons during MD is specific to binocular visual cortex, a region where contralateral and ipsilateral eye inputs converge. BD can also promote retractions suggesting that this response is primarily deprivation-induced and that visual activity from the ipsilateral eye is not required. MD in monocular visual cortex, which only receives input from the contralateral eye, produced a transient decrease in branch tip dynamics wherein branch tip elongations and retractions remained balanced in L2/3. While lid suture during MD and BD both result in the loss of visual input, this loss of visual drive does not result in a decrease in thalamic firing but rather a decrease in correlated activity (Linden, Heynen et al. 2009). Uncorrelated activity has been demonstrated to be a key trigger in the activity-dependent weakening of divergent inputs during development (Hata and Stryker 1994; Hata, Tsumoto et al. 1999; Frenkel and Bear 2004; Haruta and Hata 2007). Since MD in monocular visual cortex and BD in binocular visual cortex should both produce a cortical environment absent of visual input and dominated by uncorrelated activity, the different structural dynamics in these regions suggest that uncorrelated activity by itself is not sufficient to explain these differences. However, it seems clear that the anatomical presence of ipsilateral eye input is necessary to produce the L2/3 branch tip retractions observed in binocular visual cortex during BD and MD.

Functional Consequences of Interneuron Dendritic Arbor Remodeling

We find that MD in binocular visual cortex produces a total branch tip length change of $32.7 \pm 5.7 \mu\text{m}$ per cell or $1.81 \pm 0.31\%$ of the total branch tip length per cell. Measurements by electron microscopy have indicated that the synaptic density of L2/3 interneuron dendrites is approximately 1 synapse per μm (Kubota, Karube et al. 2007).

We estimate that the synaptic turnover associated with these structural rearrangements during MD is on the order of ~30 synapses or ~2% of dendritic synapses per cell. This is a minimal estimate of total synaptic turnover for each interneuron as synapse dynamics on stable dendrites during MD have not been measured. Never-the-less, this estimate of synapse turnover is slightly lower but on the same order of fractional dendritic spine turnover of ~5-10% observed in L5 pyramidal neurons during MD in visual cortex (Hofer, Mrsic-Flogel et al. 2009) or during behavioral motor learning in motor cortex (Xu, Yu et al. 2009; Yang, Pan et al. 2009), suggesting that the dynamics of structurally-related synaptic remodelling that occurs in the adult cortex during plasticity is comparable between excitatory and inhibitory cell types.

Local networks in L2/3 are largely composed of local pyramidal-interneuron-pyramidal connections (Holmgren, Harkany et al. 2003). About 80% of the synapses on distal interneuron dendrites represent excitatory connections (Kubota, Karube et al. 2007). These excitatory connections are comprised of a large number of local pyramidal neurons that each makes relatively few (3-7) synaptic connections (Markram, Toledo-Rodriguez et al. 2004). It is estimated that as few as 10 pre-synaptic, temporally correlated excitatory inputs are sufficient to trigger an action potential in inhibitory cells (Buhl, Tamas et al. 1997). For bitufted interneurons, a train of action potentials from even a single synaptic contact can produce an action potential (Kaiser, Lubke et al. 2004). Thus, a total branch tip length change of ~30 μm (or ~30 synapses) per cell could potentially alter the connectivity of 5-10 excitatory pre-synaptic partners, each with significant ability to initiate interneuron firing. Furthermore, one inhibitory cell makes a large number (15-20) of synapses on to local excitatory cells despite representing only about 20% of cortical neurons. As a result, the activity of a given

post-synaptic cell can be more strongly influenced by the minority of inhibitory neurons that synapse onto it than by the excitatory majority. Changes to dendritic inputs of interneurons could thus have a widespread influence upon its post-synaptic targets and activity of local cortical circuitry. While the degree of structurally-related synaptic changes may be similar between excitatory and inhibitory neurons, the functional consequences of these changes might be profoundly different.

It is also important to consider that while the change in total branch tip length per cell in binocular visual cortex during MD increased by ~ 1.5 fold, the fraction of individual dynamic branch tips per cell increased by ~ 3 fold. Our observation that the average length change per branch tip was unaffected by MD suggests that MD primarily increases the number of dynamic branch tips in a given cell. It has been proposed that structural plasticity in the adult brain serves to increase the number of potential synaptic contacts by increasing spatial access to distinct circuits within an arbor's vicinity (Chklovskii, Mel et al. 2004). For example, it is estimated that the geometry and space occupied by each dendritic spine in mouse cortex is capable of making approximately 4 potential synaptic contacts (Stepanyants, Hof et al. 2002). An entire dendritic branch tip likely contains an even higher number of possible synaptic connections considering its shape and observed changes in length. By the same rationale, further increasing an interneuron's potential for sampling distinct circuits would be more readily achieved by modest length changes in several branch tips spatially distributed throughout the dendritic field as compared to a substantial length change of a single branch tip. Our data would suggest that interneuron dendritic arbor remodeling functions to access and alter connectivity between different circuits in cortical space. This is supported by the cortical and laminar specificity of these rearrangements, arguing for a circuit-specific

form of rewiring. Any synaptic weight changes associated with the loss or gain of synapses during a branch tip retraction or elongation, while interrelated, may be secondary consequences of these wiring changes. We speculate that changes in the balance between elongations and retractions can serve as an indicator for more global synaptic events occurring throughout the cell such as synapse turnover on stable arbors.

Structurally-Mediated Disinhibition as a Mechanism for Adult Brain Plasticity

Given the predominance of excitatory synapses on interneuron dendrites, we propose that the initial branch tip retractions induced by 4 days of BD or MD results in reducing the contribution of excitatory drive to interneurons, producing a period of disinhibition in the local circuit. The lack of dendritic spine loss in excitatory pyramidal neurons to balance these interneuron retractions could potentially enhance the effects of this reduced inhibition. Reduced inhibition, in turn, enables the strengthening of non-deprived eye inputs between 4 to 7 days of MD as represented by interneuron branch tip elongations in L2/3 as well as dendritic spine formation in L5 pyramidal neurons (Hofer, Mrsic-Flogel et al. 2009).

In support of the relationship between branch tip retraction and disinhibition, we demonstrate that global disinhibition by fluoxetine treatment can provide a permissive environment similar to that afforded by sensory deprivation. Since fluoxetine treatment during normal vision resulted in a balanced increase in structural dynamics, it is likely that fluoxetine does not act directly on interneurons to eliminate excitatory input, but produces disinhibition by other mechanisms allowing enhanced structural plasticity. This disinhibition when paired with a brief MD allows for the immediate strengthening of non-deprived eye connections, including branch tip elongations, resulting in a faster

functional adaptation resembling that of the developmental critical period. The maturation of inhibitory circuits during development has been demonstrated to regulate the onset and closure of critical period plasticity (Hensch, Fagiolini et al. 1998; Hanover, Huang et al. 1999; Huang, Kirkwood et al. 1999). One of the fundamental differences between critical period and adult plasticity in the mouse visual cortex is the duration of MD required to produce an OD shift (Sawtell, Frenkel et al. 2003; Hofer, Mrsic-Flogel et al. 2006; Sato and Stryker 2008). The time necessary for visual deprivation to produce the initial branch tip retractions and local disinhibition of mature interneurons may be a contributing factor to the prolonged MD required for adult OD plasticity.

Two general mechanisms have been proposed to account for the OD plasticity occurring during MD, particularly the potentiation of the non-deprived eye response. One model suggests that correlated activity from the non-deprived eye can strengthen those inputs through Hebbian forms of plasticity as represented by long-term potentiation (LTP) (Smith, Heynen et al. 2009). Another model suggests that homeostatic regulation to preserve neuronal firing rate through synaptic scaling, intrinsic excitability, or other compensatory mechanisms contributes to the strengthening of non-deprived eye responses during MD (Turrigiano 2008). Our findings could potentially be relevant to both mechanisms. Reduction of GABA-mediated inhibition in slice preparations as well as after fluoxetine treatment has been shown to facilitate the induction of LTP in L2/3 of adult visual cortex (Artola and Singer 1987; Kirkwood and Bear 1994; Maya Vetencourt, Sale et al. 2008). The reduced inhibition produced by interneuron dendrite retraction may provide more salience to patterned visual activity from the non-deprived eye enabling a Hebbian-

based strengthening of non-deprived eye connections which could include the branch tip elongations observed. The possibility that these later elongations may represent a homeostatic response to the initial retractions to maintain firing rates within each interneuron seems unlikely since branch tip retractions during BD are not balanced by subsequent elongations. Despite this, the overall effect of disinhibition in response to reduced visual activity during deprivation could contribute to homeostatic regulation to preserve cortical activity across the network.

The consequence of strengthening non-deprived eye input onto both pyramidal neurons and interneurons would be reestablishment of excitatory drive onto these interneurons, thus restoring inhibition to the local circuit. Similar to what has been observed in the auditory cortex (Froemke, Merzenich et al. 2007), this rebalancing of excitation/inhibition may bring the window of plasticity afforded by disinhibition to a close, contributing to the saturation in both structural and OD plasticity observed after 7d MD. In this respect, the plasticity of inhibitory circuits serves as a form of homeostatic regulation, triggering both the beginning and end of functional as well as structural adaptation.

Interneuron Dendritic Arbor Remodeling is Specific to Novel Experiences

Increasing evidence suggests that structural rearrangements are primarily induced by novel experiences. Dendritic spine dynamics in the adult motor cortex increased only during naïve training to specific motor tasks as opposed to retraining of the same tasks learned earlier in life (Xu, Yu et al. 2009). Similarly, dendritic spine gain was only observed in the adult visual cortex during an initial MD and not during a repeated MD (Hofer, Mrsic-Flogel et al. 2009). These initial structural changes can

persist from weeks to months, long after the functional expression of these modifications become suppressed such as during recovery or post-training (Linkenhoker, von der Ohe et al. 2005; Hofer, Mrsic-Flogel et al. 2009; Yang, Pan et al. 2009). It is thought that these lasting structural changes can contribute to rapid functional adaptations upon re-exposure to the same sensory manipulation or during re-learning (Knudsen 2002; Hofer, Mrsic-Flogel et al. 2006). The observed interneuron branch tip dynamics, which was specifically induced during a first MD and not during recovery or a second MD, lends further evidence to the idea that structural plasticity functions during novel experience to establish connections that can be readily be reactivated in response to repeated experiences.

Laminar-Specific Dendritic Branch Tip Rearrangements Balances Influence of Feedforward vs. Feedback Inputs

Of additional interest, we find that changes in experience can differentially alter branch tips dynamics for arbors extending into L1 versus L2/3. While it has been shown that different propensities for structural plasticity exist for dendritic spines on pyramidal neurons based on their somatic location within cortical laminae (De Paola, Holtmaat et al. 2006; Chow, Groszer et al. 2009; Hofer, Mrsic-Flogel et al. 2009), this is the first evidence demonstrating laminar differences in experience-dependent remodeling of interneuron branch tips. In the non-human primate visual system, superficial L2/3 has been identified as a region where bottom-up feedforward sensory inputs arriving in L2/3 (Nassi and Callaway 2009) converge with top-down feedback inputs modulating attention, response strength, and saliency arriving in L1 (Rockland and Pandya 1979; Maunsell and van Essen 1983; Bullier, Hupe et al. 2001). These

anatomical pathways have also been shown to exist in the mouse visual cortex (Antonini, Fagiolini et al. 1999; Yamashita, Valkova et al. 2003; Dong, Shao et al. 2004; Dong, Wang et al. 2004). While the functional interactions between these two pathways have not been as extensively studied in the rodent visual system, there is evidence suggesting that feedforward and feedback inputs make distinct connections onto inhibitory neurons in superficial L2/3 with each form of input eliciting different synaptic responses (Gonchar and Burkhalter 2003; Yamashita, Valkova et al. 2003; Dong, Shao et al. 2004; Dong, Wang et al. 2004). Thus, laminar-specific reorganization of interneuron dendritic arbors could affect the relative influence of feedforward and feedback input on the local inhibitory network, in turn affecting the relative contribution of bottom-up or top-down processing of visual information. It was reported that MD in adult mice can lead to enhanced vision in the non-deprived eye (Prusky, Alam et al. 2006; Fischer, Graves et al. 2007). The pathway-specific capacity for remodeling in superficial L2/3 interneurons could aid in balancing the relative contribution of different visual streams in order to maintain or improve vision in the face of a changing environment.

Conclusions

Our findings support a role for disinhibition in experience-dependent plasticity and provide a potential structural mechanism that would facilitate circuit-specific modifications. They further suggest that therapeutic approaches that reduce cortical inhibition are effective only in combination with an instructive stimulus. While fluoxetine treatment does not afford the same circuit-specific disinhibition as deprivation, with appropriately selective input it could nevertheless prove effective in

enhancing cognitive abilities and restoring function to fully developed circuits impaired by neurological damage or disease.

METHODS

Surgical Procedure and Fluoxetine Administration

To allow long-term visualization of *in vivo* neuronal morphology cranial windows were bilaterally implanted over the visual cortices of adult *thyl*-GFP-S mice (postnatal days 42-57) as previously described (Lee, Chen et al. 2008). Sulfamethoxazole (1 mg/ml) and trimethoprim (0.2 mg/ml) were chronically administered in the drinking water through the final imaging session to maintain optical clarity of implanted windows. For animals subjected to fluoxetine treatment, fluoxetine-hydrochloride (160 mg/L) was chronically administered in the drinking water with Sulfamethoxazole (6 mg/tablet) and Trimethoprim (1 mg/tablet) supplemented in the food pellet (Bio-Serv).

Two-Photon Imaging

Starting at three weeks after cranial window surgery, allowing sufficient time for recovery, adult mice were anesthetized with 1.25% avertin (7.5 ml/kg IP). Anaesthesia was monitored by breathing rate and foot pinch reflex and additional doses of anaesthetic were administered during the imaging session as needed. *In vivo* two-photon imaging was performed using a custom-built microscope modified for *in vivo* imaging by including a custom-made stereotaxic restraint affixed to a stage insert and custom

acquisition software. The light source for two-photon excitation was a commercial Mai Tai HP Ti:Sapphire laser (Spectra-Physics) pumped by a 14-W solid state laser delivering 100 fs pulses at a rate of 80 MHz with the power delivered to the objective ranging from approximately 37–50 mW depending on imaging depth. Z-resolution was obtained with a piezo actuator positioning system (Piezosystem Jena) mounted to the objective. The excitation wavelength was set to 950 nm, with the excitation signal passing through a 20x/1.0 NA water immersion objective (Plan-Apochromat, Zeiss) and collected after a barrier filter by a photomultiplier tube. Given the sparse density of GFP expression in the *thy1*-GFP-S line, typically only one cell (with a maximum of two) was imaged per animal.

Optical Intrinsic Signal Imaging

For functional identification of monocular and binocular visual cortex, optical imaging of intrinsic signal and data analysis were performed as described previously (Kalatsky and Stryker 2003). Mice were anesthetized and maintained on 0.5-0.8% isoflurane supplemented by chlorprothixene (10 mg/kg, i.m.), and placed in a stereotaxic frame. The heart rate was continuously monitored through electrocardiograph leads attached to the animal. For visual stimuli, a horizontal bar (5° in height and 73° in width) drifting up with a period of 12 seconds was presented for 60 cycles on a high-refresh-rate monitor positioned 25 cm in front of the animal. Optical images of visual cortex were acquired continuously under a 610 nm illumination with an intrinsic imaging system (LongDaq Imager 3001/C; Optical Imaging Inc.) and a 2.5x/0.075 NA (Zeiss) objective. Images were spatially binned by 4x4 pixels for analysis. Cortical intrinsic signal was obtained by extracting the Fourier component of

light reflectance changes matched to the stimulus frequency whereby the magnitudes of response in these maps are fractional changes in reflectance. The magnitude maps were threshold at 30% of peak response amplitude to define a response region. Primary visual cortex was determined by stimulation of both eyes. Binocular visual cortex was determined by stimulation of the ipsilateral eye. Monocular visual cortex was determined by subtracting the map of binocular visual cortex from the map of primary visual cortex.

Monocular and Binocular Deprivation

Monocular and binocular deprivation were performed by eyelid suture. Mice were anesthetized by 1.25% avertin (7.5 ml/kg IP). Lid margins were trimmed and triple antibiotic ophthalmic ointment (Bausch & Lomb) was applied to the eye. Three to five mattress stitches were placed using 6-0 vicryl along the extent of the trimmed lids. Animals whose eyelids did not seal fully shut were excluded from further experiments.

Transneuronal Labeling of Thalamocortical Projections

Wheat germ agglutinin-Alexa555 conjugate (100mg/mL, 2–3 μ l; Molecular Probes) in saline was injected into the ipsilateral eye. After 3–5 d post-injection, animals were anesthetized with 1.25% avertin (7.5 ml/kg IP) and perfused transcardially with 4% paraformaldehyde (PFA) in phosphate buffer, pH 7.4. The brain was extracted and fixed overnight in 4% PFA. Seventy-five micrometer-thick coronal sections were cut from the visual cortex using a vibratome (Leica VT100; Leica). Sections were subsequently incubated with 4'6-diamidino-2-phenylindole (DAPI) (1:1,000; Sigma) before mounting and visualization. Imaged cells were identified by

location, morphology, and local landmarks. Images were acquired with an upright epifluorescence scope using a 1x/0.04 NA, 10x/0.30 NA, or 20 x/0.75 NA objective (Nikon).

Data Analysis

Using Matlab (Mathworks) and ImageJ (National Institutes of Health), 16-bit two-photon raw scanner data was converted into an 8-bit image z-stack for dendrite reconstruction and analysis in Neurolucida (MicroBrightField, Inc.). For each individual cell, 4-D (x, y, z, and t) stacks were traced and analyzed blind to age. Branch tips (segments of dendrite from the branch point to the terminal) were analyzed and Fano Factor (FF) values for were obtained as previously described (Lee, Chen et al. 2008). Only branch tips with terminals that could be confidently identified across all imaging sessions, not extending beyond the imaging volume, or obscured by blood vessels were monitored and included in analysis. Monitored branch tips with $FF > 1.09$, representing the 1.5*interquartile range above the upper quartile of the sample population were identified, confirmed as dynamic by visual examination, and subjected to further analysis. The mean FF across all monitored branch tips for each superficial L2/3 interneuron was calculated to confirm that each cell met the threshold (mean $FF > 0.35$) previously determined for a dynamic cell. In total, 1470 monitored dendritic branch tips out of 1536 total branch tips from 44 cells from 42 animals were followed over 6-7 imaging sessions. For each cell, the percentage of branch tips elongating or retracting between two successive imaging sessions relative to the total branch tip number of the previous imaging session, were defined as the rates of branch tip elongations and retractions, respectively. Elongations and retractions included both the

elongations and retractions of existing branch tips as well as the addition and elimination of entire branch tips. Rate of branch tip dynamics was defined as the sum of the rates of branch tip elongations and retractions. The depth of each dynamic branch tip was determined from analysis of the imaging volume data in *Neuroleucida* based on its position relative to the soma, with the soma depth measured by z-stack position relative to the pial surface and verified by post-hoc DAPI staining showing the L1-L2/3 border at ~65um below the pial surface.

FIGURES

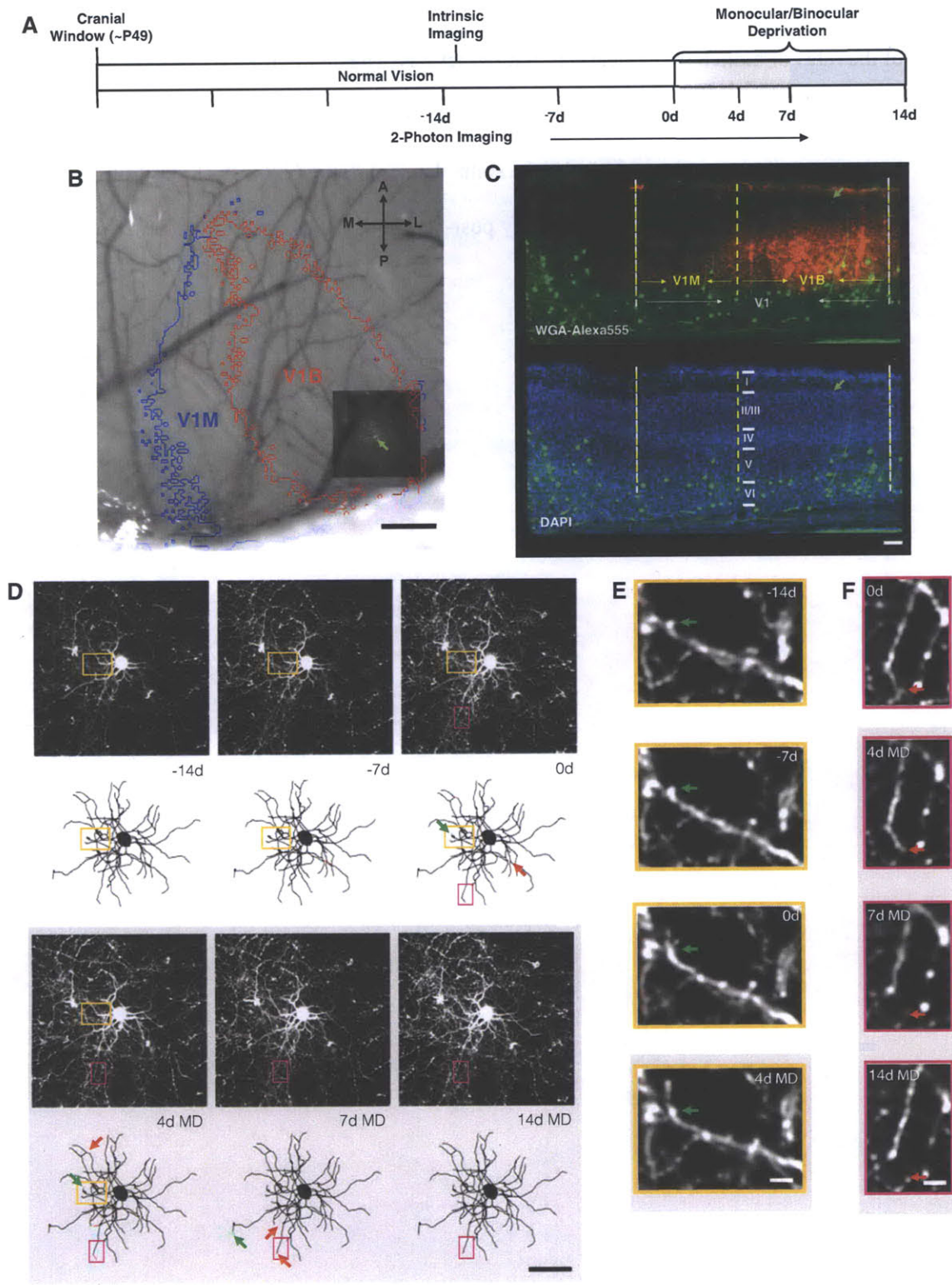


Figure 1. Chronic Two-Photon *In Vivo* Imaging of Dendritic Branch Tip Dynamics in Superficial L2/3 Cortical Interneurons (A) Experimental time course. Every cell was imaged at all time points. (B) Maximum z-projection (MZP) of chronically imaged interneuron (green arrow) superimposed over intrinsic signal map of monocular (V1M) and binocular (V1B) visual cortex. (C) Coronal section of primary visual cortex (V1) containing an imaged superficial L2/3 interneuron (~70 μm below the pial surface) (green arrow) shown with respect to V1M and V1B as identified through WGA-Alexa555 labeling of thalamocortical projections from the ipsilateral eye (red) and DAPI staining of the granule cell layer (blue). (D) MZPs near the cell body (above) along with two-dimensional projections of three-dimensional skeletal reconstructions (below) of a superficial L2/3 interneuron (~85 μm below the pial surface) in V1B acquired at the specified intervals. Dendritic branch tip elongations and retractions identified between successive imaging sessions are indicated by green and red arrows, respectively. (E) High-magnification view of one branch tip elongation (orange box in [D]). Green arrow marks the approximate distal end of the branch tip at -14d. (F) High-magnification view of one branch tip retraction (magenta box in [D]). Red arrow marks the approximate distal end of the branch tip at 0d. Scale bars: (B), 250 μm ; (C), 100 μm ; (D), 50 μm ; (E and F), 5 μm .

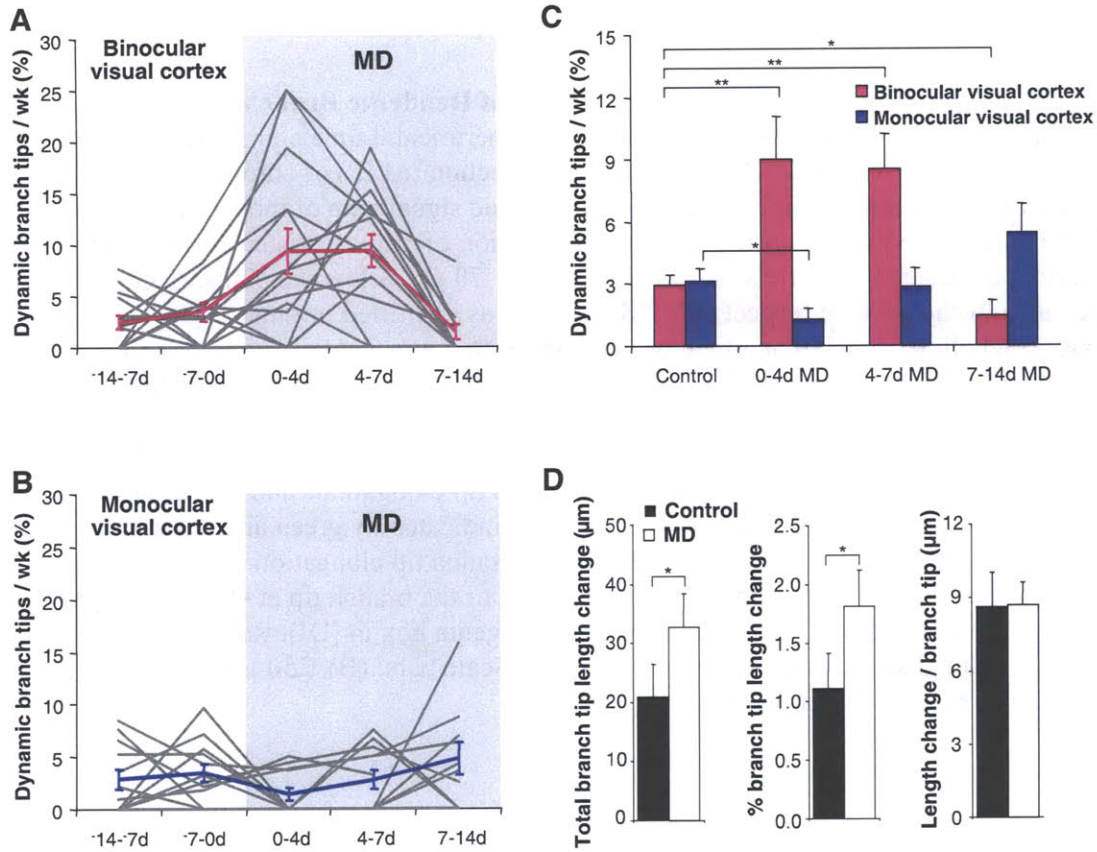


Figure 2. Monocular Deprivation Increases Interneuron Dendritic Branch Tip Dynamics in Adult Binocular Visual Cortex (A-B) Dendritic branch tip dynamics in superficial L2/3 interneurons imaged throughout a 14 day MD for: (A) binocular visual cortex, individual cells shown in grey, mean shown in magenta. ($n = 16$ cells from 13 mice, 524 branch tips) and; (B) monocular visual cortex, individual cells shown in grey, mean shown in blue. ($n = 12$ cells from 12 mice, 461 branch tips). (C) Rate of dendritic branch tip dynamics compared before and during MD in binocular (magenta) and monocular (blue) visual cortex. (D) Quantification of branch tip length changes in binocular visual cortex before and during MD: total branch tip length change per cell (right), percent of total branch tip length change per cell (middle), length change per branch tip (left). (** $p < 0.01$, * $p < 0.05$). Error bars, s.e.m.

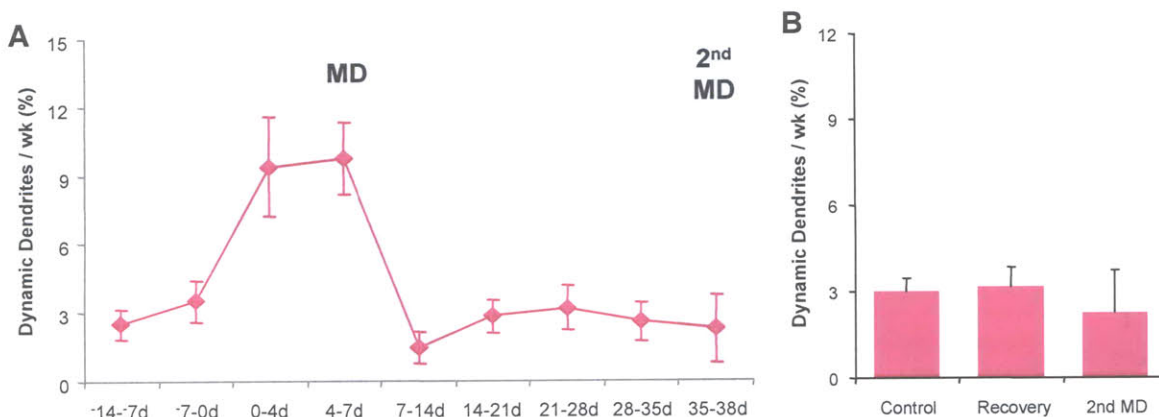


Figure 3. Recovery and Repeated MD does not Increase Branch Tip Dynamics in Adult Binocular Visual Cortex (A) Dendritic branch tip dynamics in superficial L2/3 interneurons imaged through a 14 day MD, 3 weeks of recovery, and a second 3 day MD. (B) Rate of dendritic branch tip dynamics compared during recovery and second MD in binocular visual cortex. (control, n = 16 cells from 13 mice, 524 branch tips; recovery, n = 11 cells from 11 mice, 366 branch tips; second MD, n = 7 cells from 7 mice, 269 branch tips). Error bars, s.e.m.

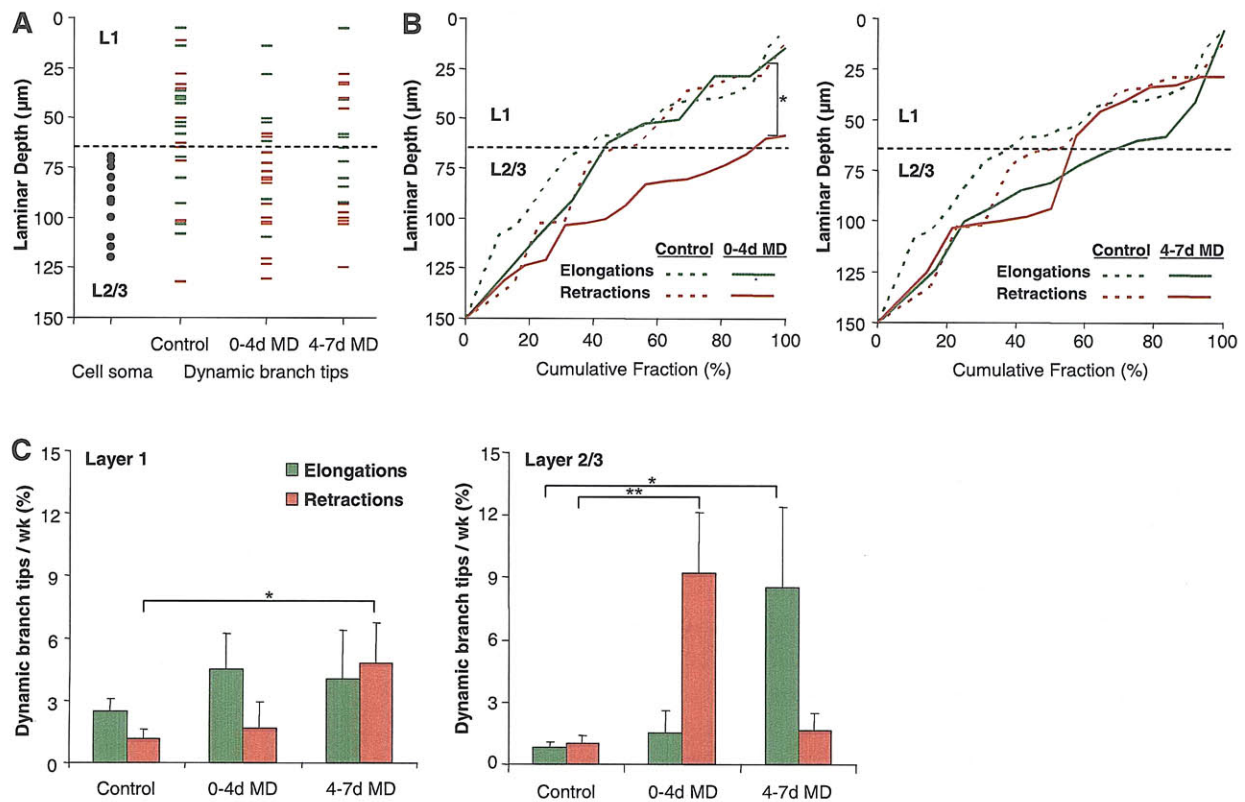


Figure 4. Monocular Deprivation Induces Laminar Specific Dendritic Arbor Rearrangements (A) Distribution of dynamic branch tips before and during MD in binocular visual cortex. Plotted are cell soma positions (black circles) and branch tips positions of branch tip elongations (green) or retractions (red). (B) Cumulative fraction distribution plot of branch tip elongations (green) and retractions (red) at 0-4d MD (left) and 4-7d MD (right) as compared to control (dotted lines) (* $p < 0.05$). (C) Rate of dendritic branch tip elongations (green) and retractions (red) in L1 and L2/3 of binocular visual cortex, before and during MD. (n = 16 cells from 13 mice, L1: 228 branch tips. L2/3: 325 branch tips) (** $p < 0.01$, * $p < 0.05$). Error bars, s.e.m.

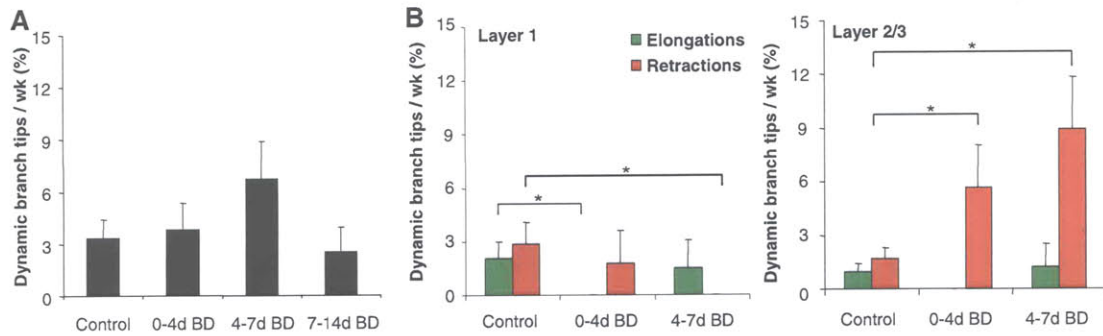


Figure 5. Binocular Deprivation Specifically Increases Retractions of L2/3 Branch Tips (A) Dendritic branch tip dynamics compared before and during BD in binocular visual cortex. (B) Rate of branch tip elongations (green) and retractions (red) in L1 and L2/3 of binocular visual cortex, before and during BD. (n = 7 cells from 7 mice, L1: 108 branch tips. L2/3: 155 branch tips) (** p < 0.02, * p < 0.05). Error bars, s.e.m.

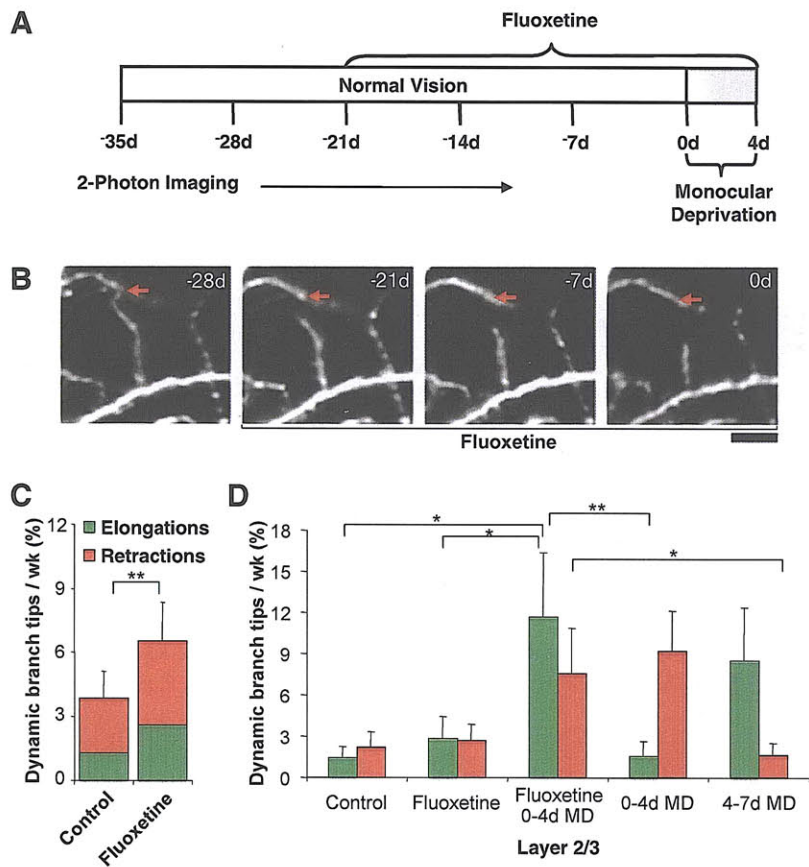


Figure 6. Reduction in Intracortical Inhibition by Fluoxetine Treatment Promotes Experience-Dependent Branch Tip Remodeling (A) Experimental time course. (B) High-magnification view of one branch tip retraction during fluoxetine treatment. Red arrow marks the approximate distal end of the branch tip at -28d. Scale bar: 10 μm . (C) Dendritic branch tip dynamics in binocular visual cortex of animals under normal vision before and during fluoxetine administration. ($n = 8$ cells from 8 mice, 228 branch tips) (D) Rates of L2/3 branch tip elongations and retractions in binocular visual cortex during fluoxetine treatment under normal vision or a brief 4d MD as compared to prolonged 7d MD without fluoxetine treatment. (with fluoxetine, $n = 8$ cells from 8 mice, L2/3: 115 branch tips; without fluoxetine, $n = 16$ cells from 13 mice, L2/3: 325 branch tips). (** $p < 0.01$; * $p < 0.05$). Error bars, s.e.m.

SUPPLEMENTAL DATA

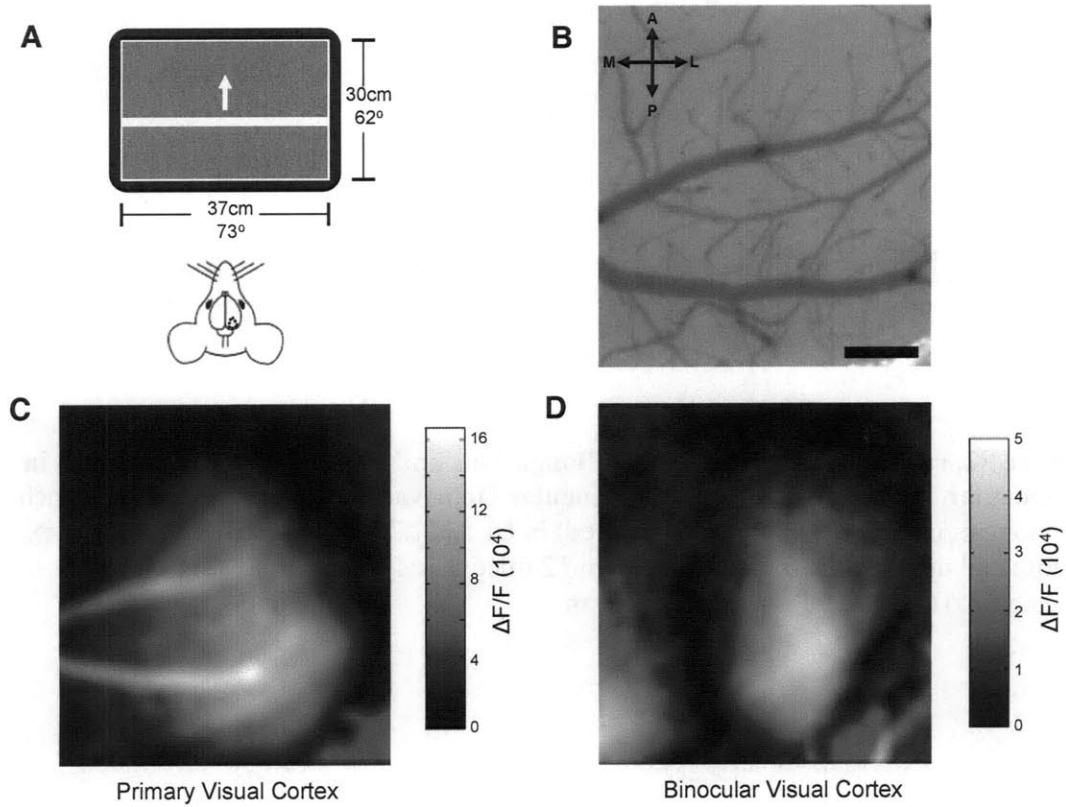


Figure 1. Late *In Utero* Lentiviral Injections Selectively Labels Excitatory Neurons in Superficial Cortical Layers (A) Epifluorescent image of 75 μ m coronal section from adult mouse that received a late *in utero* (E16) injection of FUGW into the lateral ventricle. GFP positive cells (in white) are uniformly distributed along the cortex with propidium iodide staining (in red) detailing the cortical lamina. (B) High magnification view showing selective labeling in cortical layer 2/3. (C) Robust GFP expression is seen in excitatory neurons, effectively labeling dendritic arbors. Scale bars: (A), 100 μ m; (B), 100 μ m; (C), 50 μ m.

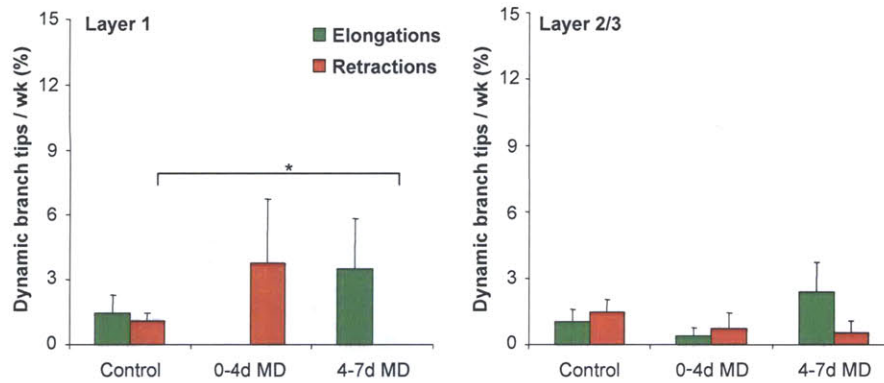


Figure S2, related to Figure 4. L2/3 Elongations and Retractions are Balanced in Monocular Visual Cortex during Monocular Deprivation Rates of dendritic branch tip elongations (green) and retractions (red) in L1 and L2/3 of monocular visual cortex, before and during MD. (n = 12 cells from 12 mice, L1: 196 branch tips. L2/3: 291 branch tips) (* p < 0.05). Error bars, s.e.m.

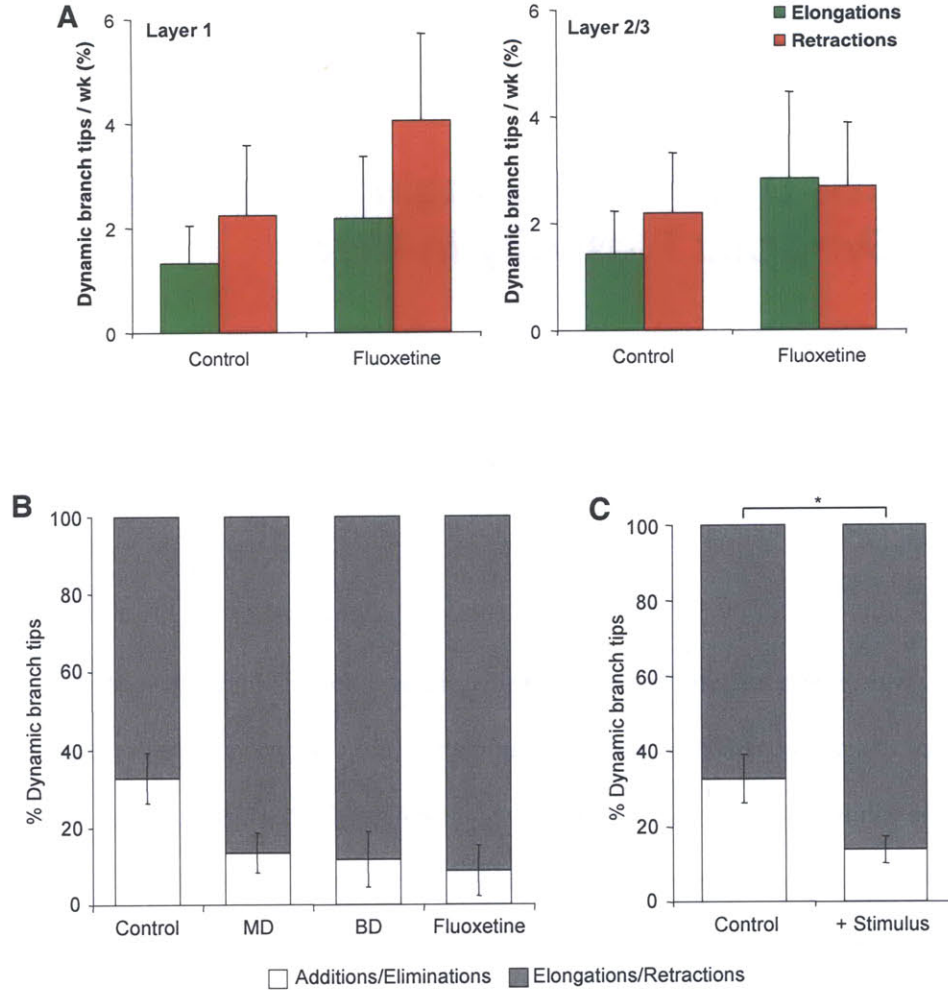


Figure S3, related to Figure 6. Further Analysis of Branch Tip Dynamics During Fluoxetine Treatment (A) Rates of dendritic branch tip elongations (green) and retractions (red) in binocular visual cortex before and during fluoxetine treatment under normal vision in L1 and L2/3. (n = 8 cells from 8 mice, L1: 113 branch tips. L2/3: 115 branch tips) (B) Comparison between elongations/retractions of existing branch tips versus additions/eliminations (elongations/retractions of entire branch tips) of entire branch tips during MD, BD, and fluoxetine treatment in binocular visual cortex. (C) Comparison between elongations/retractions of existing branch tips versus additions/eliminations (elongations/retractions of entire branch tips) across all visual or pharmacological stimuli presented in (b). (n = 44 cells from 42 animals, Mann-Whitney *U*-test, * $p < 0.02$). Error bars, s.e.m.

CHAPTER 3

Towards Dual Color Imaging of Structural and Synaptic Plasticity *In Vivo*

ABSTRACT

In vivo two-photon imaging has begun to shed light on how changes in experience can produce structural changes in the adult mammalian brain. However, it is not known how the formation and elimination of individual synapses accompany these structural modifications. In order to address this question, we present a technique to simultaneously monitor structural and synaptic dynamics in the *in vivo* mammalian cortex. Structural and synaptic components can be labeled in cortical neurons of mice in a cell type and laminar specific manner through co-injection of independent lentiviral vectors at a late embryonic or early postnatal age. We demonstrate that excitatory and inhibitory post-synaptic densities can be visualized by tagging fluorescent proteins to PSD95 and Gephyrin, respectively. Finally, we show that the fluorescent proteins, Teal and Venus, can be simultaneously excited and spectrally resolved through linear unmixing so that individual structural and synaptic components can be identified and followed over time. Through this approach, the relationship between synaptic and structural plasticity can be studied in the living brain.

INTRODUCTION

It is thought that the structural changes that contribute to experience-dependent plasticity in the brain are accompanied by the formation or elimination of synaptic connections (Bailey and Kandel 1993). The development of two-photon microscopy (Denk, Strickler et al. 1990) along with transgenic and viral-mediated gene delivery technologies to achieve stable, sparse fluorescent labeling of neuronal structures (Feng, Mellor et al. 2000; Dittgen, Nimmerjahn et al. 2004) has created the possibility of studying structural plasticity in the mammalian brain. While these studies have shed light on how changes in sensory experience can alter structural dynamics (Holtmaat and Svoboda 2009), clear discrepancies between exist between observed structural rearrangements and the synaptic plasticity presumed to accompany it. In addition, while particular attention has been focused on the *in vivo* dynamics of dendritic spines and axonal boutons as they represent one-to-one estimates of synaptic turnover, the dynamics of other types of connections such as dendritic shaft, peri-somatic, and axo-axonic synapses remain unaccounted for. Thus, the structural dynamics observed so far may underestimate the degree of synaptic reorganization occurring within the adult brain.

In order to address these and related questions concerning the relationship between structural and synaptic plasticity, methods to simultaneously image structural and synaptic dynamics need to be implemented. This can be achieved by employing spectrally resolvable fluorophores to tag molecules normally localized to specific structural or synaptic elements. *In vivo* two-photon imaging studies using this approach have generally been limited to species such as the developing xenopus tadpole

(Ruthazer, Li et al. 2006) or zebrafish larvae (Niell, Meyer et al. 2004) where light absorbance and scatter is minimal. Simultaneous imaging of structural and synaptic dynamics has been performed in the mammalian brain using two separate two-photon light sources to achieve optimal excitation of distinct fluorophores (Gray, Weimer et al. 2006). However, this strategy is not ideal for extending the technique to multi-color imaging of multiple structural and synaptic components. Given these current limitations, we investigated whether chronic *in vivo* two-photon imaging of structural and synaptic dynamics can be performed in the mammalian brain using spectrally resolvable fluorophores that could be efficiently and simultaneously excited with a single two-photon excitation source.

RESULTS

Laminar and Cell Type Specific Targeting of Cortical Neurons through *In Utero* or Early Postnatal Lentiviral Delivery

In order to label structural and synaptic components for chronic *in vivo* two-photon imaging, genetic manipulation of neuronal populations must be achieved in a cell type and laminar specific manner. L2/3 pyramidal neurons can be selectively targeted by performing *in utero* electroporation of plasmids into the lateral ventricle at an embryonic time point when neuroblasts that later give rise to these neurons line the ventricular zone (Tabata and Nakajima 2001). To test a variation of this approach, we injected a lentiviral vector expressing GFP (FUGW) (Lois, Hong et al. 2002) into the lateral ventricle of E16.5 mouse embryos to achieve stable but minimal overexpression

of GFP. This resulted in a uniformly distributed labeling of L2/3 pyramidal neurons in the adult cortex, amenable for single-cell two-photon imaging (Figure 1A-C).

L2/3 interneurons can also be selectively labeled *in utero* by targeted electroporation of plasmids (Borrell, Yoshimura et al. 2005) or ultrasound-guided delivery of viral vectors (Stott and Kirik 2006) into the ganglionic eminence. While ultrasound-guided injections were not attempted, targeted electroporation into the ganglionic eminence proved problematic. Labeling L2/3 interneurons requires that targeted *in utero* electroporations be performed at E13.5 when embryos are more susceptible to premature abortions, particularly in the C57Bl/6 background mouse line often used for visual system and plasticity studies. Abortions can be avoided to a degree by electroporating a fraction of the total embryos within a pregnant animal. However, once they are born, it becomes difficult to distinguish which pups have been labeled so they can be selected for further studies. Thus, the overall effort with this approach can be met with very low success rates.

Given this complication, an early postnatal lentiviral delivery strategy was explored. Mice from P4-P6 received an injection of FUGW directly into cortical L2/3. Later inspections of coronal sections of adult cortex from injected animals show no apparent signs of tissue damage, suggesting that the developing cortex in early postnatal animals allows for sufficient cortical recovery for later *in vivo* imaging studies in the adult. GFP expression in the adult cortex exhibited a high density of GFP-labeled neurons near the injection site (Figure 2A). However, sparser labeling amenable for single cell two-photon imaging was seen up to 1mm away from the injection site (Figure 2B). Thus, while this technique labels both excitatory and inhibitory neurons, inhibitory neurons can be identified by morphology and isolated for studies.

Labeling Structures and Synapses through Tagged Fluorescent Proteins

In order to label different structural and synaptic components for two-photon imaging, we tested various viral constructs expressing fluorescent proteins tagged with different localization signals or to molecules normally localized to specific synaptic sites. Cytoplasmic GFP or YFP has traditionally been used for *in vivo* structural imaging. However, adequate labeling typically requires high levels of fluorescent protein expression to the cytoplasm, usually achieved in certain transgenic lines (Feng, Mellor et al. 2000) or with strong viral promoters (Dittgen, Nimmerjahn et al. 2004). Despite this, thin axonal segments can still be difficult to visualize due to the small volume of cytoplasm in those regions. As an alternative, we tested a lentiviral vector expressing Venus, a YFP variant, tagged with a C-terminal farnesylation signal for membrane localization (FUVFW). Two-photon imaging of adult animals after an early postnatal injection of FUVFW exhibited strong labeling of dendritic and axonal arbors in the cortex (Figure 3A and B). Axonal arbors could be easily followed through the imaging volume and dendritic spine morphology could also be more easily visualized.

Fluorescent tagging of PSD95, a scaffolding protein localized at excitatory post-synaptic densities (PSDs), has been used to study synapse formation on developing dendritic arbors (Niell, Meyer et al. 2004) as well as the molecule's kinetics in dendritic spines *in vivo* (Gray, Weimer et al. 2006). To determine whether this could be used as an excitatory post-synaptic marker, we performed an early postnatal injection of lentivirus expressing PSD95-GFP (FsynPSD95GFPW). *In vivo* two-photon imaging showed punctate labeling that could be visualized up ~200 μm below the pial surface. Some punctas were highly clustered, possibly corresponding to PSDs on the tips of

dendritic spines along a pyramidal neuron (Figure 3C). Other punctas were densely aligned in a linear fashion, suggesting synapse labeling of dendritic shafts of putative interneurons (Figure 3D). We also examined the possibility of using Gephyrin, a scaffolding protein found at inhibitory post-synaptic densities (Triller, Cluzaud et al. 1985; Schmitt, Knaus et al. 1987), to visualize inhibitory synapses. *In vivo* two-photon imaging of adult cortex after early postnatal injection of lentivirus expressing Teal-Gephyrin (FsynTealGephyrinW) showed sparsely distributed puncta along the dendritic shaft up to ~200 μm below the pial surface (Figure 3D). The visualization of these PSDs suggests that PSD95 and Gephyrin are adequate markers for excitatory and inhibitory synapses and that sufficient amounts of fluorescent proteins can be localized to these structures to provide enough signal for *in vivo* two-photon imaging.

Dual Gene Expression through Co-Injection of Independent Lentiviral Vectors

Visualizing structural and synaptic dynamics within the same neuron requires methods to achieve dual gene expression of fluorescently labeled structural and synaptic components. Furthermore, sufficient levels of expression are needed to attain adequate signal for *in vivo* two-photon imaging. Bicistronic lentiviral vectors have so far proven elusive to produce robust dual gene expression (Semple-Rowland, Eccles et al. 2007; Gascon, Paez-Gomez et al. 2008; Chinnasamy, Shaffer et al. 2009). As an alternative approach, we investigated whether sufficient dual gene expression could be achieved by co-infecting two independent lentiviral constructs into the same neuron. Lentiviruses FsynPSD95GFPW and FUtdTomatoW, expressing tdTomato, were volume adjusted for equal titer and injected into the cortex of early postnatal mice. Quantification of dual labeled cells in cortical sections showed that viral co-injection led to a ~10-20% co-

infection rate. The signal intensity for each label by epifluorescence microscopy was qualitatively comparable to that achieved by injection of single viruses (Figure 4). Thus, co-injection of independent lentiviral vectors provides sufficient dual gene expression for potential visualization by *in vivo* two photon imaging.

Identifying Fluorescent Partners for Dual Color Two-Photon Microscopy

In order to image and resolve individual structural and synaptic components, distinct fluorescent proteins must be identified that can be efficiently and simultaneously excited with a single two-photon light source and whose emission spectra can be fully resolved. The increasing spectral diversity of genetically-encoded fluorophores, both brighter and more amenable to two-photon excitation (Day and Davidson 2009), presented us with a few candidates for testing (Table 1). From these, potential fluorescent combinations were selected for dual color two-photon imaging. We first tested a combination of PSD95-GFP for synaptic labeling and tdTomato for structural labeling. While GFP and tdTomato exhibit little emission spectra overlap making them easily resolvable, their peak two-photon excitation wavelength differ considerably (Figure 5A and B). Using different excitation wavelengths ranging from 950nm to 1020nm, we performed *in vivo* two-photon imaging with a dual channel detection system in the adult cortex after early postnatal co-injection of FsynPSD95-GFPW and FUtdTomatoW (Figure 5C). While PSD95-GFP could be visualized at these wavelengths with some decrease in signal as the excitation wavelength was increased beyond 980nm, tdTomato labeled dendritic arbors were hard to visualize suggesting poor excitation at the wavelengths tested. While weak excitation can be compensated to some degree with increased protein expression (Gray, Weimer et al.

2006; Madisen, Zwingman et al. 2009), using such a fluorophore as a synaptic marker would be severely limited by the inherent size of a given post-synaptic density or pre-synaptic active zone, restricting the number of localized fluorescent molecules. Furthermore, concern would also exist as to whether protein overexpression might alter normal cellular function. Overall, the weak simultaneous two-photon excitation of GFP and tdTomato led us to consider other combinations of fluorophores.

Venus and Teal, a cyan fluorescent protein variant, are more amenable to simultaneous two-photon excitation but their emission spectra exhibit a degree of overlap (Figure 6A and B). Standard methods of applying bandpass filters to isolate non-overlapping emission wavelengths eliminate a large proportion of available photons from a given fluorophore that is especially critical for *in vivo* detection of small synaptic structures. In order to retain the ability to acquire a full emission spectra while being able to resolve mixed contributions to a pixel with co-localized labels, we investigated whether spectral linear unmixing could be applied to resolve Venus and Teal *in vivo* (Zimmermann 2005). A dual channel reference spectra was obtained from transfected HEK293 cell cultures expressing either Venus or Teal (Figure 6C). Analysis of the distribution of each fluorophore by channel (Figure 6D) indicated that that the contribution of each fluorophore becomes non-deterministic at low photon counts as previously observed (Davis and Shen 2007; Ducros, Moreaux et al. 2009). Despite this potential confound, we applied linear unmixing with the acquired reference spectra to *in vivo* images of neurons co-expressing PSD95-Teal and Venus simultaneously excited with a single two-photon light source. Linear unmixing separated Teal-labeled PSD95 puncta from Venus-labeled dendritic arbors and spines (Figure 7A-C). These Teal-labeled puncta co-localized with dendritic spines where PSD95 is normally localized

demonstrating that spectral linear unmixing can be used to resolve Teal and Venus labeling *in vivo*.

Chronic *In Vivo* Imaging of Structural and Synapse Dynamics

To demonstrate that chronic *in vivo* imaging of neuronal structures and synapses can be performed with this overall approach, FUVW and FsynTealGephyrinW were co-injected into the cortex of early postnatal mice. Following rearing to adulthood and cranial window implantation, a Venus and Teal-Gephyrin positive L2/3 pyramidal neuron was identified and imaged for 8 days. After linear unmixing, dendritic arbors and spines labeled with Venus and inhibitory PSDs labeled with Teal were resolved. Time-lapsed imaging showed that individual spines and inhibitory PSDs could be tracked over the time course (Figure 8). Some inhibitory PSDs were present for the entire 8 days of imaging, while others were present for at least 4 days before being eliminated. This demonstrates that individual structural and synaptic components can be visualized and followed over the course of days.

DISCUSSION

Here we present a technique to monitor structural and synaptic plasticity in the mammalian brain *in vivo*. Structural and synaptic components can be labeled in cortical neurons of mice in a cell type and laminar specific manner through co-injection of independent lentiviruses either at a late embryonic or early postnatal age. We demonstrate that excitatory and inhibitory post-synaptic densities can be visualized by

tagging fluorescent proteins to PSD95 and Gephyrin, respectively. Finally, we show that simultaneous two-photon excitation of Teal and Venus can be achieved and that linear unmixing can be applied to spectrally resolve these fluorophores so that individual structural and synaptic components can be identified and followed over time.

Studying the Relationship between Structural and Synaptic Plasticity

Simultaneous *in vivo* imaging of structural and synaptic dynamics has already provided some insight into the relationship between synaptic and structural plasticity. Fluorescently tagged PSD95 has been used to study synapse formation on developing dendritic arbors (Niell, Meyer et al. 2004) as well as the molecule's kinetics in dendritic spines *in vivo* (Gray, Weimer et al. 2006). Labeling of the pre-synaptic molecule, synaptophysin, was used to study how synaptogenesis and synaptic maturation can stabilize axon branch dynamics during development (Ruthazer, Li et al. 2006). However, a multitude of questions still remain to be addressed.

It is clear that synaptic structures such as dendritic spines and axonal boutons do not necessarily represent a one-to-one synaptic connection. For example, evidence shows that about 2-4% spines in the neocortex lack synapses (White and Rock 1980; Hersch and White 1981; Benschalom and White 1986; Arellano, Espinosa et al. 2007). New spines can require a period of up to 4 days to form a synapse and can form contacts with boutons that already contain multiple synaptic connections (Knott, Holtmaat et al. 2006). Bouton turnover is not necessarily indicative of one-to-one synaptic gain or loss as boutons can vary in their number of synaptic connections from a few to even none (White, Weinfeld et al. 2004), and both excitatory and inhibitory boutons can partner with the same dendritic spine (Jones and Powell 1969). The ability to simultaneously

monitor structural and synaptic dynamics will allow for a more quantitatively and temporally accurate assessment of the synaptic dynamics in these structures.

Simultaneous imaging in combination with manipulations in gene expression or activity will also provide mechanistic insight for when and under what conditions do single or multi-synaptic connections form in these structures.

Synapses without direct structural correlates have so far been unobservable in the mammalian brain *in vivo*. These include the high density of glutamatergic synapses lining the dendritic shafts of aspiny interneurons (Markram, Toledo-Rodriguez et al. 2004). The ability to target interneurons through early postnatal lentiviral delivery enables these synapses to be visualized through fluorescent tagging of PSD95. Through this, one can begin to study the synaptic dynamics of dendrites that remain stable and those that remodel in superficial L2/3. *In vivo* imaging of fluorescent tagged of Gephyrin now makes it possible to study the dynamics of GABAergic synapses which make dendritic shaft and peri-somatic contacts. Through this, a more comprehensive view of synaptic reorganization can be achieved in the adult brain.

Experimental Considerations and Validations

While this approach creates a considerable amount of possibilities for observing structural, synaptic, and even molecular dynamics *in vivo*, a few considerations need to be taken into account especially regarding the selection of molecules used to tag specific synaptic compartments. Each molecule can exhibit different behaviors and kinetics as they are trafficked to and from individual synapses. While PSD95 rapidly redistributes from one synapse into the dendrite and other synapses (Gray, Weimer et al. 2006), Gephyrin can form non-synaptic microclusters that can move slowly and

discontinuously along the dendrite (Maas, Tagnaouti et al. 2006). In order to avoid misidentifying non-synaptic clusters for synapses, post-hoc analysis is necessary to corroborate the *in vivo* images of labeled puncta. Serial electron microscopy reconstructions or immunofluorescence counterstaining of pre- and post-synaptic components can be used to confirm synapse identity in previously *in vivo* imaged structures. In the future, the ability to label and visualize both pre- and post-synaptic components will also aid in the identification of synapses.

While a certain level of expression is necessary to suitably visualize synaptic components that have been labeled with fluorescently tagged molecules, the concern exists that overexpression of these molecules might result in abnormal synaptic as well as structural dynamics. The limited copy number achievable with lentivirus delivery compared to other stable gene transfer approaches (Rahim, Wong et al. 2009) aids in limiting high overexpression. Despite this, examination of basic morphology or electrophysiological recordings of labeled cells need to be performed to rule out any altered phenotype. If overexpression becomes an issue, other molecules used to label the same structure could be substituted. Alternatively, a lentivirus-mediated molecular replacement strategy (Schluter, Xu et al. 2006) can be used where a lentiviral vector can be engineered to express an RNAi hairpin to knockdown endogenous gene expression while expressing a version of the same gene that is both fluorescently-tagged and insensitive to knockdown.

Towards Multi-Color Imaging of Multiple Structural and Synaptic Components

The ability to simultaneously excite and spectrally resolve Teal and Venus *in vivo* as demonstrated here offers considerable promise towards being able to simultaneously monitor multiple structural and synaptic components, each labeled with a different fluorophore. First, efficient simultaneous two-photon excitation of multiple fluorophores eliminates the need to devote an excitation source with an optimal wavelength to each given label. Second, the ability to resolve fluorophores with spectral overlap increases the number of potential fluorophores that can be used for labeling different components.

Other recent developments suggest that simultaneous multi-color *in vivo* imaging can soon be possible. An ever increasing number of spectrally diverse genetically-encoded fluorophores, both brighter and more amenable to simultaneous two-photon excitation, have been generated that can be tested for suitable color combinations for *in vivo* imaging (Day and Davidson 2009). While low photon count conditions during *in vivo* imaging can produce confounds when linear unmixing is applied to resolve fluorophores with spectral overlap, other methods using estimation analysis have been developed for *in vivo* spectral resolution of fluorophores with a high degree of overlap (Ducros, Moreaux et al. 2009). This, in combination with methods for imaged-based removal of poisson shot noise and the use of segmentation analysis to eliminate single-pixel noise, can help to make spectral resolution during *in vivo* imaging routine.

The other challenge to imaging multiple structural and synaptic components is the ability to achieve multi-transgene expression in order to fluorescently label each component for imaging. While lentiviral vectors offer the cassette capacity to express

multiple transgenes, it is unclear if the multicistronic lentiviral vectors that have been developed (Semple-Rowland, Eccles et al. 2007; Gascon, Paez-Gomez et al. 2008; Chinnasamy, Shaffer et al. 2009) can achieve suitable expression for adequate visualization of each component. Transgenic mouse lines have also been developed that provide fluorescent protein expression to label neuronal structure in combination with a Cre/loxP-based cassette that allows for conditional expression of other transgenes within the same neuron (Livet, Weissman et al. 2007; Chakravarthy, Keck et al. 2008; Young, Qiu et al. 2008; Madisen, Zwingman et al. 2009). The combination of these viral-mediated and transgenic approaches might enable the introduction of multiple-labeled synaptic components in these already structurally labeled cells. Through this, an even broader range of questions can potentially be explored, from understanding the dynamics between excitatory and inhibitory synapses to the interactions between pre- and post-synaptic elements.

METHODS

Generation of Lentiviral Constructs

Untagged fluorescent proteins: mKeima (Kogure, Karasawa et al. 2006), tdTomato (Shaner, Campbell et al. 2004), mOrange (Shaner, Campbell et al. 2004), Venus (Nagai, Ibata et al. 2002), and Teal (Ai, Henderson et al. 2006) were amplified by PCR and inserted into lentivirus transfer vectors *pFUGW* (for ubiquitin promoter expression) or *pFsynGW* (for synapsin promoter expression) replacing GFP. *pFUVFW*

was generated by PCR amplification and insertion of Venus into the *pEGFP-F* (Clontech) followed by PCR amplification and insertion farnesylated-Venus in *pFUGW*. *pFsynPSD95TealW* was generated by PCR amplification of Teal and insertion into *pFsynPSD95GFPW* (Kelsch, Lin et al. 2008) replacing GFP. *pFsynTealGephyrinW* was generated by PCR amplification of GFP-Gephyrin (Fuhrmann, Kins et al. 2002) into *pFsynGW* replacing GFP followed by PCR amplification of Teal and insertion replacing GFP.

Lentivirus production, concentration and titer determination was performed as described (Coleman, Huentelman et al. 2003).

Expression in Cell Culture

HEK293 cells were grown on a 10-cm tissue culture dish to 40% confluence in Dulbecco's modified Eagle's medium (Sigma) with 10% fetal bovine serum (Sigma), and transfected with 4 µg / dish of plasmid using lipofectamine 2000 (Invitrogen).

***In Utero* Lentiviral Injection**

In utero lentivirus injections were performed on timed-pregnant C57Bl/6J mice (Jackson). Pregnancies were timed with day of plug detection as E1 and birth usually occurred on E19. L2/3 pyramidal neurons and progenitors were infected by injecting 1.5–2 µl of lentivirus (~1 x 10⁸ pfu/µl to ~5 x 10⁸ pfu/µl) into the lateral ventricle of E16.5 brains. Surgery and injection procedures were as previously described (Walsh and Cepko 1992).

Early Postnatal Cortical Lentiviral Injection

Early postnatal (P4-P6) C57Bl/6 mice were anesthetized with isofluorane/oxygen. The incision site was treated with 2.5% lidocaine/2.5% prilocaine and the skin overlying the occipital bone was resected. A small (<1mm) burr hole was made in the skull overlying the visual cortex with a dental drill. A fine beveled micropipette (Drummond, 30 μ l microcaps, pulled, broken, and beveled to 40 μ m diameter, 45° bevel) connected to a microinjector system (Nanoject II, Drummond) was mounted to a stereotaxic frame and lowered ~300 μ m below the pial surface. Pups received 300 nl of lentivirus (~1 x 10⁷ pfu/ μ l to ~5 x 10⁷ pfu/ μ l) to each hemisphere. After 30 seconds to allow diffusion into the brain, the micropipette was slowly retracted. The skin was closed with 5-0 sterile nylon sutures and glued with Vetbond (3M Corp). Pups were allowed to recover under a heating lamp for 1-2 hours and then returned to their mother.

Histology and Immunohistochemistry

Previously viral injected mice were heavily anesthetized with 2.5% Avertin (0.030 ml/g IP) and their brains processed for immunohistochemistry essentially as described (Chattopadhyaya, Di Cristo et al. 2004). Some sections were incubated with propidium iodide (1 μ g/mL, Carbiochem, San Diego, CA). Other sections were first incubated with GABA (rabbit polyclonal antibody; 1:5000; Sigma, St. Louis, Missouri, United States), followed with Alexa555 conjugated goat IgG secondary antibodies (1:400; Molecular Probes, Eugene, Oregon, United States), and finally with 4'6-diamidino-2-phenylindole (DAPI) (1:1,000; Sigma) before mounting and visualization.

Images were acquired with an upright epi-fluorescence scope using a 1x/0.04 NA, 10x/0.30 NA, or 20 x/0.75 NA objective (Nikon).

Cranial Window Surgery

To allow long-term visualization of *in vivo* neuronal structure and synaptic components, cranial windows were bilaterally implanted in adult C57Bl/6 mice that previously received lentiviral injections (postnatal days 42-57) as described (Lee, Chen et al. 2008). Sulfamethoxazole (1 mg/ml) and trimethoprim (0.2 mg/ml) were chronically administered in the drinking water through the final imaging session to maintain optical clarity of implanted windows.

Two-Photon Imaging

Starting at three weeks after cranial window surgery, allowing sufficient time for recovery, adult mice were anesthetized with 1.25% avertin (7.5 ml/kg IP). Anaesthesia was monitored by breathing rate and foot pinch reflex and additional doses of anaesthetic were administered during the imaging session as needed. *In vivo* two-photon imaging was performed using a custom-built microscope modified for dual channel *in vivo* imaging by including a custom-made stereotaxic restraint affixed to a stage insert and custom acquisition software. The light source for two-photon excitation was a commercial Mai Tai HP Ti:Sapphire laser (Spectra-Physics) pumped by a 14-W solid state laser delivering 100 fs pulses at a rate of 80 MHz with the power delivered to the objective ranging from approximately 37–50 mW depending on imaging depth. Z-resolution was obtained with a piezo actuator positioning system (Piezosystem Jena) mounted to the objective. The excitation wavelength ranged from 880 to 1020 nm, with

the excitation signal passing through a 20x/1.0 NA water immersion objective (Plan-Apochromat, Zeiss). After exclusion of excitation light source by barrier filter, emission photons were spectrally separated by a dichroic mirror followed by additional bandpass filters before being collected by two independent photomultiplier tubes.

Spectral Linear Unmixing and Image Analysis

Spectral linear unmixing makes the assumption that the total photon count recorded at each pixel in a given channel is the linear sum of the spectral contribution of each fluorophore weighted by their abundance. For a dual channel detection system, the contribution of two fluorophores can be represented by the following equations:

$$J_1(x,y) = s_{1,1} \times I_1(x,y) + s_{1,2} \times I_2(x,y) \quad (1)$$

$$J_2(x,y) = s_{2,1} \times I_1(x,y) + s_{2,2} \times I_2(x,y) \quad (2)$$

where J is the total signal per channel, I is the fluorophore abundance, and S is the contribution of that fluorophore. These equations can be expressed as a matrix:

$$[J] = [S] [I] \quad (3)$$

whereby the unmixed image $[I]$ can be calculated using the inverse matrix of $[S]$:

$$[I] = [S]^{-1} [J] \quad (4)$$

Assuming the detected signal in both channels represents the total spectral contribution for both fluorophores:

$$s_{1,1} + s_{2,1} = 1 \quad (5)$$

$$s_{1,2} + s_{2,2} = 1 \quad (6)$$

[S] was determined experimentally by dual channel acquisition of single excitation two-photon images of cell culture with single fluorophore expression, adjusting laser power and dwell time to achieve photon count levels approximating *in vivo* signal intensity. The mean contribution for each fluorophore into each channel representing the reference spectra from the acquired images was calculated using Matlab (Mathworks). These values were subsequently used for spectral linear unmixing of dual channel two-photon *in vivo* images using Matlab, followed by contrast adjustment in ImageJ (National Institutes of Health).

FIGURES

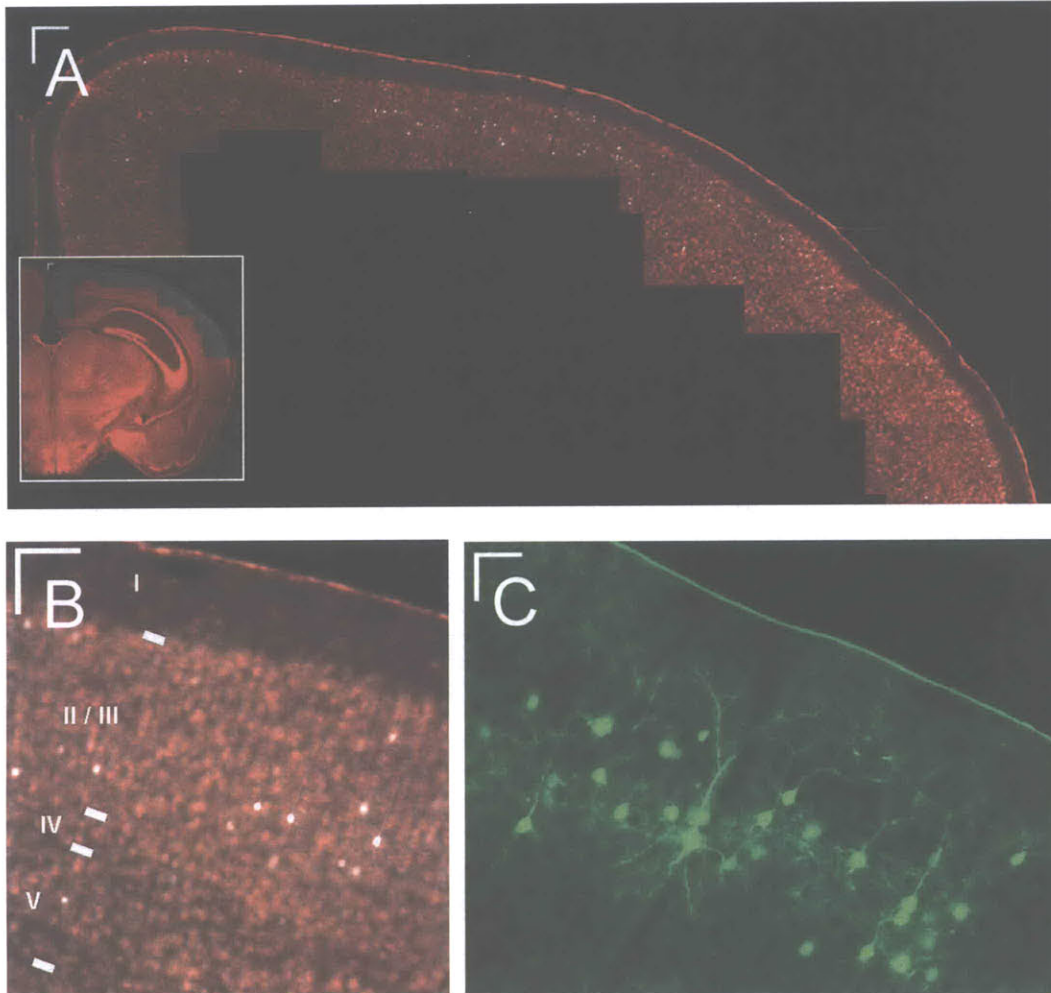


Figure 1. Late *In Utero* Lentiviral Injections Selectively Labels Excitatory Neurons in Superficial Cortical Layers (A) Epifluorescent image of 75 μm coronal section from adult mouse that received a late *in utero* (E16) injection of FUGW into the lateral ventricle. GFP positive cells (in white) are uniformly distributed along the cortex with propidium iodide staining (in red) detailing the cortical lamina. (B) High magnification view showing selective labeling in cortical layer 2/3. (C) Robust GFP expression is seen in excitatory neurons, effectively labeling dendritic arbors. Scale bars: (A), 100 μm; (B), 100 μm; (C), 50 μm.

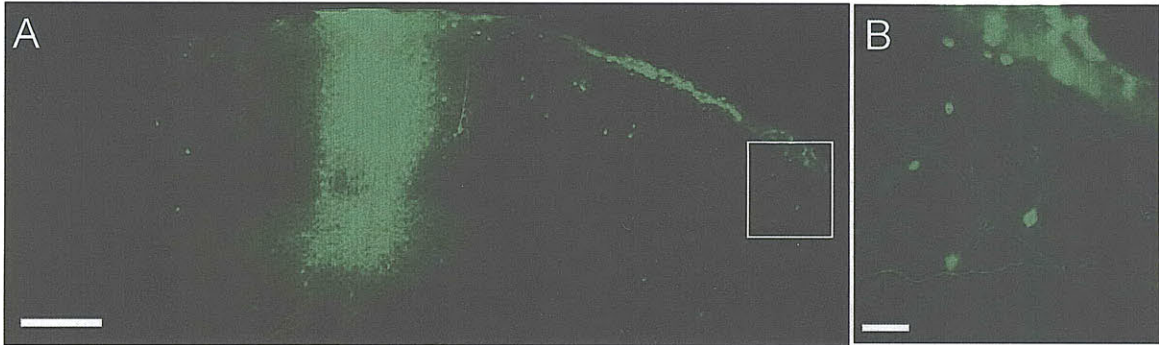


Figure 2. Early Postnatal Cortical Lentiviral Injections Labels Both Excitatory and Inhibitory Neurons (A) Epifluorescent image of 75µm coronal section from adult mouse that received an early postnatal (P4) injection of FUGW. High density of GFP-labeled excitatory and inhibitory neurons are seen at the injection site with sparser labeling seen up to 1mm from the injection site. (B) High magnification view of region outlined in white demonstrating suitable expression density for single-cell two-photon imaging. Scale bars: (A), 250 µm; (B), 100 µm.

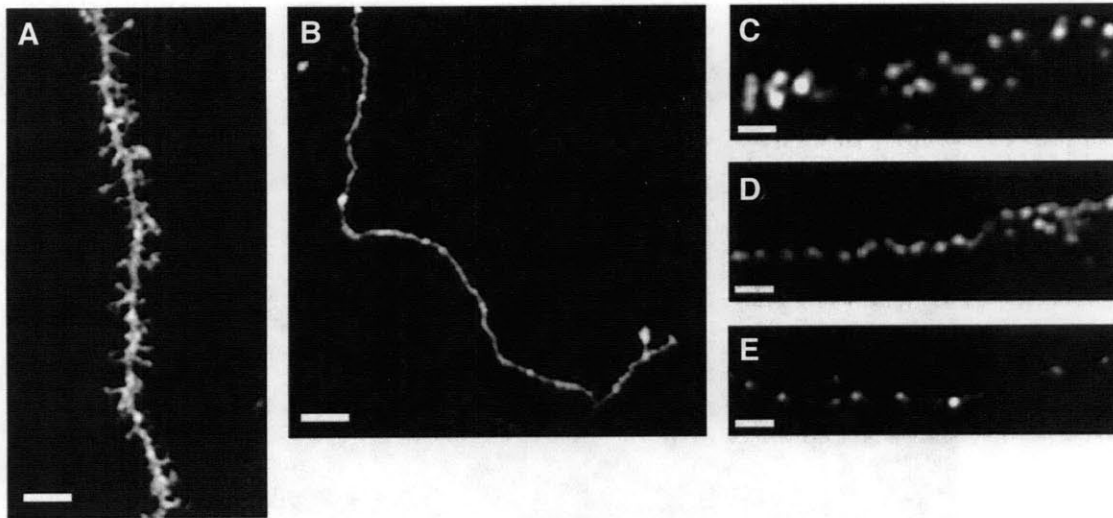


Figure 3. *In Vivo* Labeling Structural and Synaptic Components Using Tagged Fluorescent Proteins *In vivo* two-photon images of (A) Dendritic arbor and spine labeling by farnesylated-Venus. (B) Axonal arbor labeling by farnesylated-Venus. (C) Excitatory post-synaptic density labeling by PSD95-GFP along a putative pyramidal neuron dendrite. (D) Excitatory post-synaptic density labeling by PSD95-GFP along a putative interneuron dendrite. (E) Inhibitory post-synaptic density labeling by Teal-Gephyrin along a putative dendrite. Scale bars: (A-B), 5 μm ; (C-E), 2 μm .

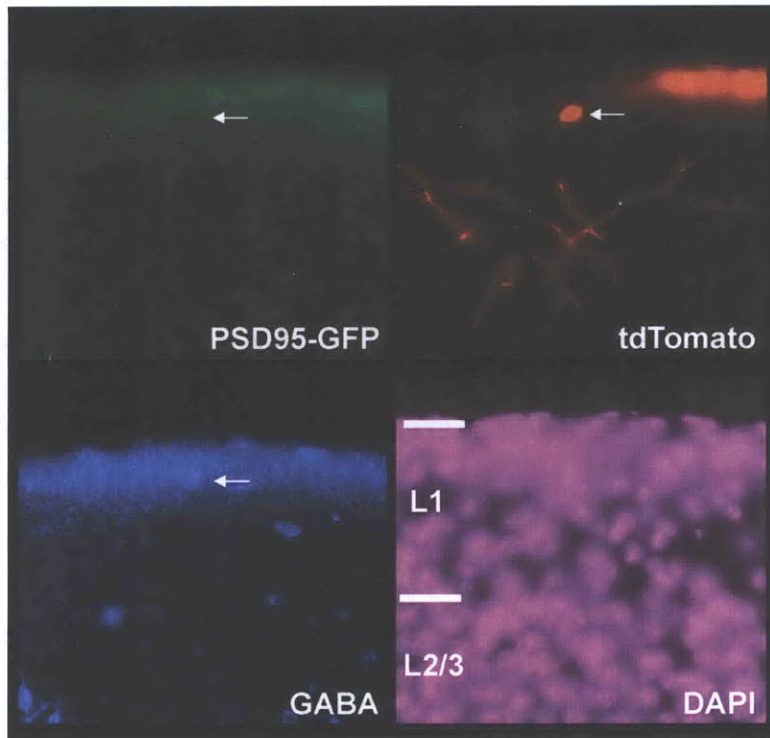


Figure 4. Cortical Lentiviral Co-Injection Yields Dual Gene Expression

Epifluorescent image of GABAergic interneuron expressing PSD95-GFP and tdTomato. Dual gene expression was obtained by co-injection of independent lentiviral vectors, FsynPSD95-GFPW and another FUtTomatoW. PSD95-GFP (upper-right panel) and tdTomato (upper-left panel) expression are shown along with anti-GABA immunostaining (lower-right panel) and DAPI staining (bottom-right panel) detailing laminar position.

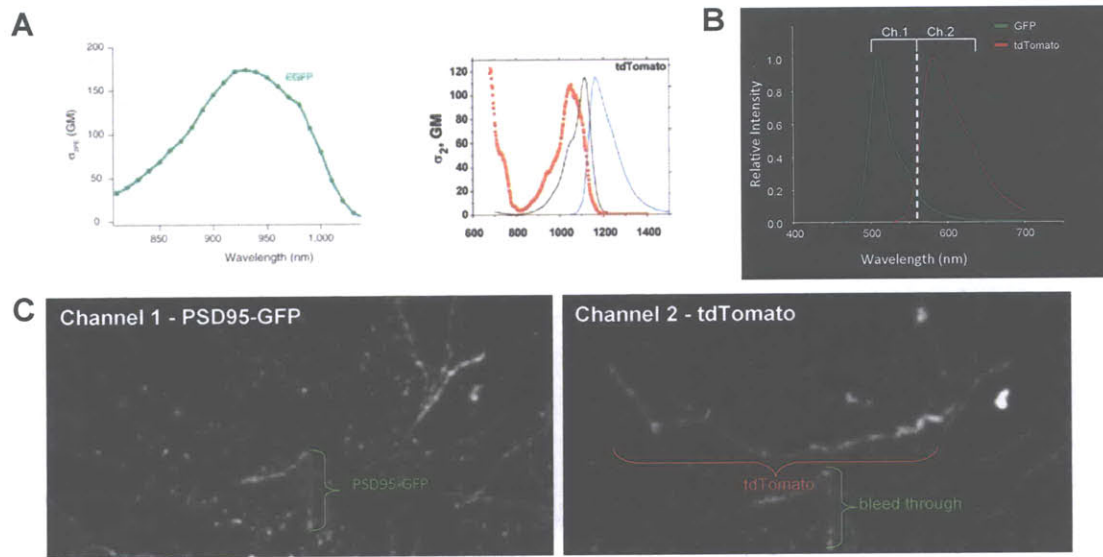


Figure 5. GFP and tdTomato are Poorly Excited with a Single Two-Photon Excitation Source (A) Two-photon excitation spectra for GFP from (Kawano, Kogure et al. 2008) and tdTomato (red dots) from (Drobizhev, Tillo et al. 2009) (B) Detection scheme for simultaneous two-photon imaging of GFP and tdTomato. Emission photons are separated with a 560nm dichroic mirror and collected into two independent PMT detectors after an additional bandpass filter at 525/50nm (Channel 1) and 605/75nm (Channel 2). (C) *In vivo* dual channel two-photon microscope image of cortical neurons expressing PSD95-GFP (left panel) and tdTomato (right panel) after lentiviral co-injection simultaneously excited with a single two-photon excitation beam at 980nm.

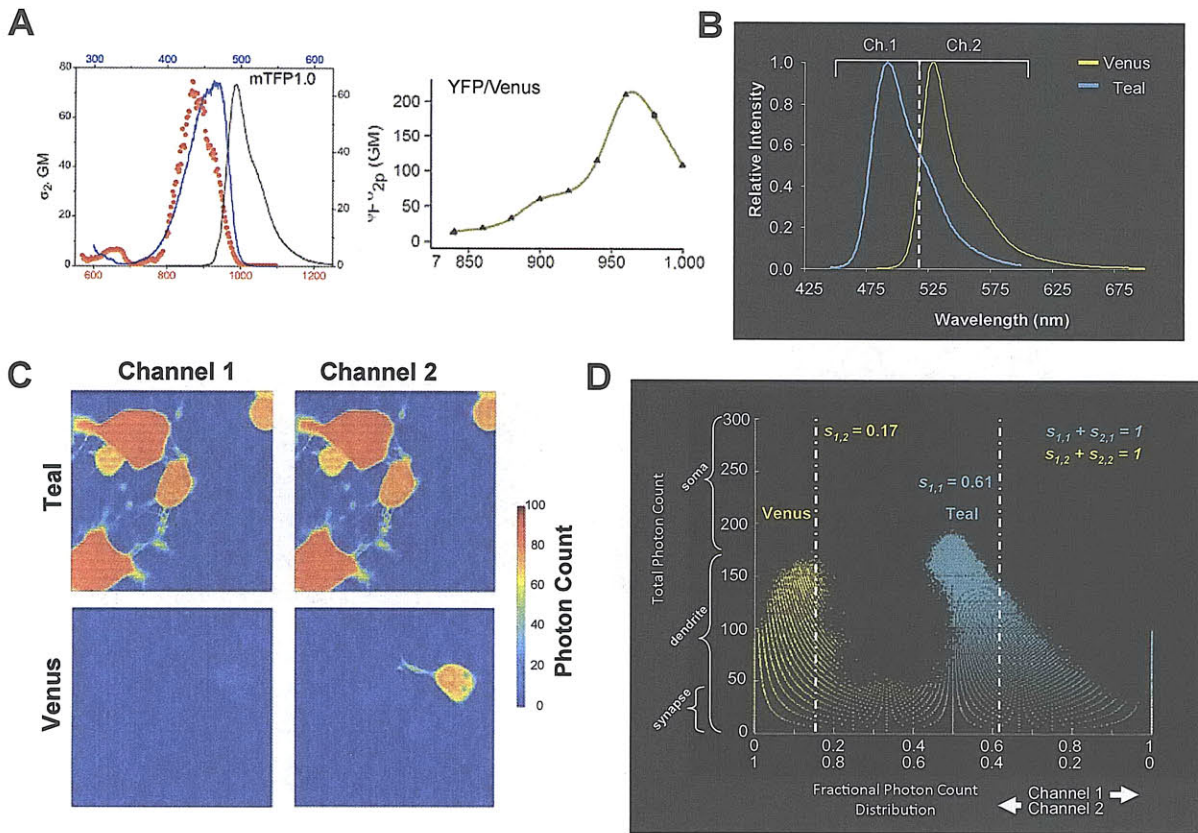


Figure 6. Teal and Venus Can Be Excited With a Single Two-Photon Excitation Source and Resolved with Spectral Linear Unmixing (A) Two-photon excitation spectra of Teal (red dots) from (Tillo, Hughes et al. 2010) and YFP/Venus from (Zipfel, Williams et al. 2003) (B) Detection scheme for simultaneous two-photon imaging of Teal and Venus fluorescent proteins. Emission spectra for Teal and Venus are split with a 520nm dichroic mirror and collected into two independent PMT detectors after an additional bandpass filter at 485/70nm (Channel 1) and 560/80nm (Channel 2). (C) Color intensity map of dual channel two-photon images of HEK293 cells expressing either Teal (above) or Venus (below). Two-photon excitation was performed at 920nm and fluorescence emission was collected using the detection scheme described in (b). (D) Experimental determination of reference spectra for spectral linear unmixing based on pure image samples shown in (c).

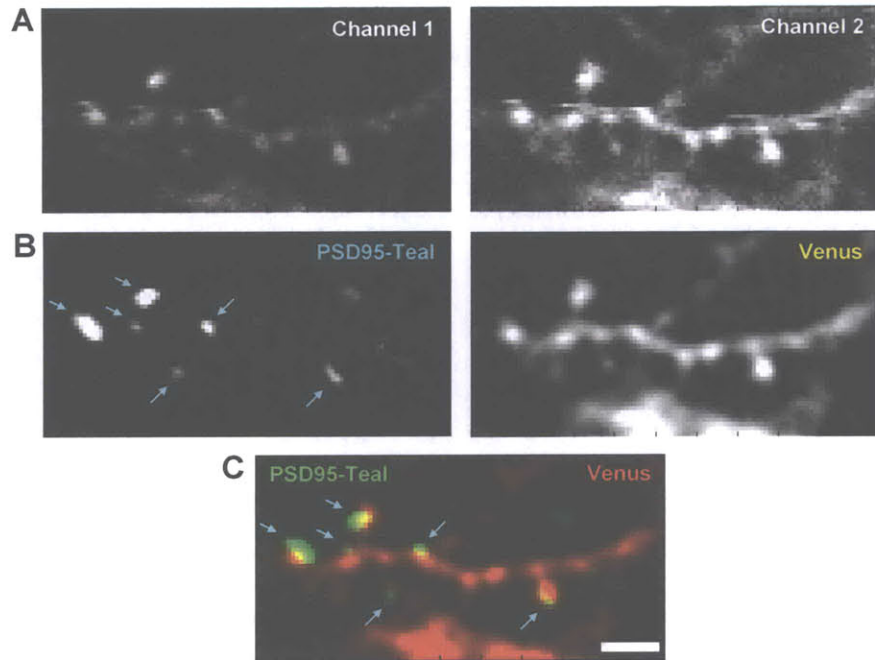


Figure 7. *In Vivo* Imaging Synaptic and Structural Components by Single Two-Photon Excitation and Spectral Linear Unmixing (A) *In vivo* dual channel images of a dendrite co-expressing PSD95-Teal and Venus after excitation with a single two-photon excitation beam at 920nm and images collected using the detection scheme described in Figure 6B. (B) PSD95-Teal (left) and Venus (right) images following spectral linear unmixing using coefficients determined in Fig. 6D. Excitatory post-synaptic densities labeled by PSD95-Teal are indicated with blue arrows. (C) Merged image from (b) showing co-localization of PSD95-Teal with dendrite spines labeled with Venus. Scale bar: 2 μ m.

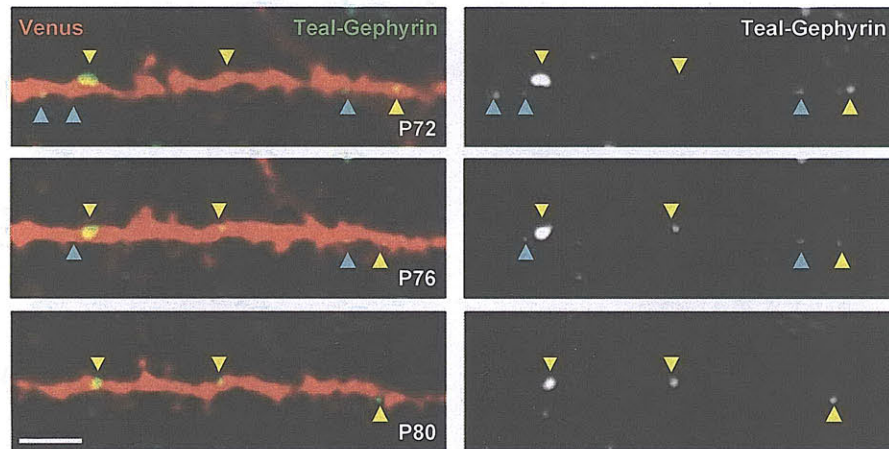


Figure 8. Chronic *In Vivo* Imaging of Inhibitory Synapses in the Adult Cortex
 Chronic *in vivo* dual color two-photon images of Teal-Gephyrin, labeling the inhibitory post-synaptic density, and Venus, labeling the dendrite, in the adult mouse cortex taken at 4 day intervals. Merged images after spectral unmixing are shown on the left with respective single channel image of Teal-Gephyrin shown on the right. Yellow arrows indicate inhibitory post-synaptic densities stable throughout all imaging sessions. Blue arrows indicate inhibitory post-synaptic densities gained or loss over the course of the imaging time course. Scale bar: 5 μ m.

TABLES

Gene	Promoter	Localization	Excitation Wavelengths (nm)	Suitable Visualization
mKeima	Ubiquitin	Cytoplasm	890-920	No
tdTomato	Ubiquitin	Cytoplasm	950-1020	No
mOrange	Synapsin	Cytoplasm	950-980	No
Venus	Ubiquitin	Cytoplasm	910-980	Yes
Teal	Ubiquitin	Cytoplasm	880-920	Yes
GFP	Ubiquitin	Cytoplasm	890-980	Yes
Venus-Farnesylated	Ubiquitin	Membrane	910-980	Yes
PSD95-GFP	Synapsin	Excitatory Synapse	890-980	Yes
PSD95-Teal	Synapsin	Excitatory Synapse	880-920	Yes
Teal-Gephyrin	Synapsin	Inhibitory Synapse	880-920	Yes

Table 1. Summary of Lentiviral Vectors Tested for *In Vivo* Two-Photon Imaging of Synaptic and Structural Components

CHAPTER 4

Conclusion

During development, extensive experience-dependent remodeling of neuronal structures is necessary for the establishment and refinement of cortical circuits. In the adult, drastic neuronal remodeling may be unnecessary for certain circuits and could in fact be detrimental to normal cognitive function (Chow, Groszer et al. 2009; Matter, Pribadi et al. 2009). However, the capacity for structural changes is still needed for recovery and functional adaptation due to stroke or peripheral injury as well as during specific learning-induced experiences (Holtmaat and Svoboda 2009). Thus, structural plasticity in the adult must not be abolished but tightly regulated. Our findings describe a direct and reciprocal regulatory relationship between structural and inhibitory-mediated plasticity that would enable specific long-lasting changes to occur in the adult cortex.

STRUCTURAL AND INHIBITORY-MEDIATED PLASTICITY IN THE ADULT CORTEX

Using *in vivo* two photon microscopy, we monitored dendritic branch tip remodeling in superficial L2/3 interneurons during experience-dependent plasticity in the adult mouse visual cortex. While visual deprivation has been shown to reduce levels of GABAergic inhibition in the adult visual cortex (Hendry and Jones 1986;

Hendry and Jones 1988; Hendry, Fuchs et al. 1990; Hendry, Huntsman et al. 1994; He, Hodos et al. 2006), we demonstrate that this is accompanied by laminar and circuit-specific retractions of interneuron branch tips providing a mechanistic link between changes in sensory activity and the resulting loss in intracortical inhibition. The attractive feature of a structural mechanism for changes in inhibitory tone is that inhibition could be altered and regulated in a highly local and restrictive manner.

Disinhibition provides a permissive environment to facilitate strengthening of salient inputs such as the potentiation of the non-deprived eye response during MD and to restore cortical plasticity in the adult to a juvenile state (Harauzov, Spolidoro et al. 2010). Increasing evidence demonstrates that structural plasticity appears to be one major component of this inhibitory-mediated effect. It is thought that the extracellular matrix (ECM), which is composed of a variety of interconnected molecules filling the space between cells in the brain, can limit structural plasticity in the adult brain (Dityatev and Schachner 2003). Proteolysis of the ECM by tissue plasminogen activator has been shown to be necessary for dendritic spine motility during development (Mataga, Mizuguchi et al. 2004; Oray, Majewska et al. 2004). Chondroitin sulphate proteoglycans (CSPGs) are one of the molecules that make up the ECM and are a major component of perineuronal nets (PNNs) which enwrap parvalbumin positive-interneurons (Hartig, Derouiche et al. 1999). The disruption of PNNs can lead to the reduction of perisomatic inhibition in targeted cells (Saghatelian, Dityatev et al. 2001). The degradation of CSPGs by chondroitinase ABC (chABC) has been shown to breakdown PNNs and reactivates OD plasticity in the adult visual cortex (Pizzorusso, Medini et al. 2002). It also enables dendritic spine growth to occur during adult recovery from a juvenile MD (Pizzorusso, Medini et al. 2006). Interestingly, the

normal expression of CSPGs can be regulated by levels of intracortical inhibition (Harauzov, Spolidoro et al. 2010). In the context of our findings, this suggests that the disinhibition produced by branch tip retractions during monocular deprivation could elicit a set of molecular mechanisms which would enable ECM reorganization to allow the formation of new connections to take place such as branch tip elongations and dendritic spine formation during OD plasticity.

This relationship between structural and inhibitory-mediated plasticity in the adult extends beyond sensory deprivation. Environmental enrichment can also produce a reduction in inhibitory tone and density of PNNs (Sale, Maya Vetencourt et al. 2007) with accompanied increases in dendritic spine dynamics (Yang, Pan et al. 2009). We observed increases in dendritic arbor dynamics upon the pharmacological administration of the anti-depressant, fluoxetine, which also reduces intracortical inhibition (Maya Vetencourt, Sale et al. 2008). These findings raise the possibility that this relationship can be exploited in situations where cognitive deficits could be restored by rebalancing excitation and inhibition (Rubenstein and Merzenich 2003; Kleschevnikov, Belichenko et al. 2004; Dani, Chang et al. 2005; Fernandez, Morishita et al. 2007) or where structural plasticity needs to be promoted for recovery from stroke or injury.

While it is clear that sensory deprivation produces interneuron branch tip retractions, the mechanism for this induction remains elusive. The robust depression in deprived-eye response in this cell type during MD (Kameyama, Sohya et al. 2010) suggests that these structural modifications represent the removal of input with reduced sensory activity. However, the presence of retractions during binocular deprivation suggests that the imbalance of eye inputs thought to initiate OD plasticity (Wiesel and

Hubel 1965) does not appear to be what is producing these changes. It is also not necessarily apparent if these retractions represent some sort of homeostatic response (Turrigiano 2008) to the loss of visual drive since MD does not produce similar branch tip dynamics in binocular and monocular visual cortex. Understanding the activity-regulated mechanisms for interneuron branch tip remodeling is critical for understanding how these changes might function during other forms of experience-dependent plasticity such as perceptual learning where plasticity is primarily induced by instructive stimuli as opposed as to the absence of sensory input. The location of these interneurons in superficial L2/3 and the evidence for L1 and L2/3 specific remodeling again make them appealing potential participants in perceptual learning, which is thought to be heavily dependent upon top-down processing (Gilbert 1998). While perceptual learning occurs through a range of timescales, branch tip remodeling might have influences on a variety of interneuron-dependent processes from the shaping of receptive fields to cortical dynamics based on different brain states that would contribute to learning (Alitto and Dan 2010). Undoubtedly, there are numerous avenues of potential investigation that could be pursued to assess the role of these structural rearrangements beyond its contribution to cortical excitatory-inhibitory balance.

NOVEL AND LEARNED EXPERIENCES IN THE ADULT CORTEX

We find that branch tip dynamics are specifically increased during novel experiences in the adult cortex. Novel experiences appear to be a common feature that can produce structural changes during both sensory deprivation and behavioral learning.

Dendritic spine dynamics in the adult motor cortex increase only during naïve training to specific motor tasks as opposed to retraining of the same tasks learned earlier in life (Xu, Yu et al. 2009). Similarly, dendritic spine gain was only observed in the adult visual cortex during an initial MD and not during a repeated MD (Hofer, Mrsic-Flogel et al. 2009). These initial structural changes can persist from weeks to months, long after the functional expression of these modifications become suppressed such as during recovery or post-training (Linkenhoker, von der Ohe et al. 2005; Hofer, Mrsic-Flogel et al. 2009; Yang, Pan et al. 2009). It is thought that these lasting structural changes can contribute to rapid functional adaptations upon re-exposure to the same sensory manipulation or during re-learning (Knudsen 2002; Hofer, Mrsic-Flogel et al. 2006), thus potentially distinguishing structural plasticity from other forms of neuronal plasticity in the adult brain.

As a point of digression, these findings raise an interesting question as to what makes an experience novel in order for it to produce structural changes in primary sensory areas. While the duration of a novel experience up to a saturation point is necessary to produce structural changes that are long lasting as in the case of a prolonged 7 day MD or 4 days of repeated behavior learning, structural changes can still be induced upon a single behavioral training session (Xu, Yu et al. 2009). It is somewhat surprising that the brain immediately “recognizes” that it must rearrange its connections in response to something it has never experienced before compared to something it experienced weeks or months earlier. One can argue that the basic sensory input arriving from the periphery that represents a previous experience and a novel experience should be the same. However from the evidence of us and others, one underlying difference between these situations is the connectivity pattern in a cortical

circuit experiencing some sensory input for the first time versus a circuit re-experiencing that identical sensory input. While those particular differences in connections, which one can define as a memory, may be inactive or suppressed at the time of re-exposure, it suggests that these differences may come into play as sensory information is being processed, ultimately producing different cortical representations of the same sensory experience. From this perspective, the recognition of novelty might arise from the mismatch between the cortical representation produced by an unlearned and learned state of connectivity. Thus, that structural plasticity is driven by changes in sensory activity at a given point in time might not be the entire part of the story. Instead, one can think of structural plasticity as an ongoing effort for the brain to achieve a state of connectivity that represents not only its current sensory experience but also its entire history of experiences as well.

FUTURE EXPERIMENTS

In order to understand the full extent and significance that interneuron dendritic remodeling and other structural rearrangements can contribute to adult cortical plasticity, an examination of the synaptic events accompanying these structural changes must be performed. Armed with the ability to simultaneously monitor structural and synaptic plasticity *in vivo* as described in Chapter 3, the following questions can be addressed:

How Does Synaptic Plasticity Accompany Interneuron Dendritic Arbor

Remodeling?

Serial EM reconstructions of interneuron dendrites have revealed a synaptic density of ~ 1 synapse per μm , $\sim 80\%$ of which are excitatory (Kubota, Karube et al. 2007). Thus, one of the primary consequences of dendritic branch tip remodeling is the reorganization of excitatory input onto these cells. By labeling excitatory synapses with PSD95-Teal and dendrites with Venus in superficial L2/3 interneurons, the relationship between these components can be assessed during experience-dependent plasticity. One can determine whether synapses are added or eliminated in an all-or-none or sequential fashion as a branch tip elongates or retracts. One can address if synaptic dynamics on a branch tip is predictive of the branch tip's subsequent behaviour. One can also determine the extent to which excitatory synapse turnover occurs on stable dendritic arbors. Through this, a more complete characterization of the synaptic dynamics in this cell type can be achieved.

Do GABAergic Synapses Mediate Local Dendritic Spine Plasticity?

Another question arising from the studies reported here is how might changes in excitatory input in superficial L2/3 interneurons specifically alter GABAergic synapse dynamics on targeted cells. Superficial L2/3 interneurons make a range of connections onto local cortical neurons including L2/3 pyramidal neurons and the apical dendrites of L5 pyramidal neurons (Markram, Toledo-Rodriguez et al. 2004). Monocular deprivation increased spine gain in L5 apical dendrites but not L2/3 pyramidal neurons in the adult visual cortex (Hofer, Mrsic-Flogel et al. 2009). This suggests that GABAergic synapse dynamics on pyramidal neurons during adult OD plasticity might

also follow laminar and cell type specific rules. By labeling inhibitory synapses with Teal-Gephyrin and dendrites with Venus in L2/3 or L5 pyramidal neurons, GABAergic synapse dynamics in these cell types can be assessed during experience-dependent plasticity. Since reductions in inhibitory tone enable the strengthening of the non-deprived eye during OD plasticity, one would predict that GABAergic synapse elimination might precede dendritic spine formation in binocular visual cortex in response to MD. By monitoring both GABAergic synapse and dendritic spine dynamics on the same portion of dendrite, one can ask if inhibitory synapses can mediate structural plasticity in a local manner.

References

- Ai, H. W., J. N. Henderson, et al. (2006). "Directed evolution of a monomeric, bright and photostable version of Clavularia cyan fluorescent protein: structural characterization and applications in fluorescence imaging." Biochem J **400**(3): 531-40.
- Alitto, H. J. and Y. Dan (2010). "Function of inhibition in visual cortical processing." Curr Opin Neurobiol.
- Antonini, A., M. Fagiolini, et al. (1999). "Anatomical correlates of functional plasticity in mouse visual cortex." J Neurosci **19**(11): 4388-406.
- Arellano, J. I., A. Espinosa, et al. (2007). "Non-synaptic dendritic spines in neocortex." Neuroscience **145**(2): 464-9.
- Artola, A. and W. Singer (1987). "Long-term potentiation and NMDA receptors in rat visual cortex." Nature **330**(6149): 649-52.
- Bailey, C. H. and E. R. Kandel (1993). "Structural changes accompanying memory storage." Annu Rev Physiol **55**: 397-426.
- Benshalom, G. and E. L. White (1986). "Quantification of thalamocortical synapses with spiny stellate neurons in layer IV of mouse somatosensory cortex." J Comp Neurol **253**(3): 303-14.
- Borrell, V., Y. Yoshimura, et al. (2005). "Targeted gene delivery to telencephalic inhibitory neurons by directional in utero electroporation." J Neurosci Methods **143**(2): 151-8.
- Buhl, E. H., G. Tamas, et al. (1997). "Effect, number and location of synapses made by single pyramidal cells onto aspiny interneurons of cat visual cortex." J Physiol **500 (Pt 3)**: 689-713.
- Bullier, J., J. M. Hupe, et al. (2001). "The role of feedback connections in shaping the responses of visual cortical neurons." Prog Brain Res **134**: 193-204.
- Buonomano, D. V. and M. M. Merzenich (1998). "Cortical plasticity: from synapses to maps." Annu Rev Neurosci **21**: 149-86.
- Chakravarthy, S., T. Keck, et al. (2008). "Cre-dependent expression of multiple transgenes in isolated neurons of the adult forebrain." PLoS One **3**(8): e3059.

- Chattopadhyaya, B., G. Di Cristo, et al. (2004). "Experience and activity-dependent maturation of perisomatic GABAergic innervation in primary visual cortex during a postnatal critical period." J Neurosci **24**(43): 9598-611.
- Chinnasamy, N., J. Shaffer, et al. (2009). "Production of multicistronic HIV-1 based lentiviral vectors." Methods Mol Biol **515**: 137-50.
- Chklovskii, D. B., B. W. Mel, et al. (2004). "Cortical rewiring and information storage." Nature **431**(7010): 782-8.
- Chow, D. K., M. Groszer, et al. (2009). "Laminar and compartmental regulation of dendritic growth in mature cortex." Nat Neurosci **12**(2): 116-8.
- Coleman, J. E., M. J. Huentelman, et al. (2003). "Efficient large-scale production and concentration of HIV-1-based lentiviral vectors for use in vivo." Physiol Genomics **12**(3): 221-8.
- Dani, V. S., Q. Chang, et al. (2005). "Reduced cortical activity due to a shift in the balance between excitation and inhibition in a mouse model of Rett syndrome." Proc Natl Acad Sci U S A **102**(35): 12560-5.
- Darian-Smith, C. and C. D. Gilbert (1994). "Axonal sprouting accompanies functional reorganization in adult cat striate cortex." Nature **368**(6473): 737-40.
- Davis, L. M. and G. Q. Shen (2007). "Extension of multidimensional microscopy to ultra-sensitive applications with maximum-likelihood analysis - art. no. 64430N." Three-Dimensional and Multidimensional Microscopy: Image Acquisition and Processing XIV **6443**: N4430-N443085.
- Daw, N. W., K. Fox, et al. (1992). "Critical period for monocular deprivation in the cat visual cortex." J Neurophysiol **67**(1): 197-202.
- Day, R. N. and M. W. Davidson (2009). "The fluorescent protein palette: tools for cellular imaging." Chem Soc Rev **38**(10): 2887-921.
- De Paola, V., A. Holtmaat, et al. (2006). "Cell type-specific structural plasticity of axonal branches and boutons in the adult neocortex." Neuron **49**(6): 861-75.
- Denk, W., J. H. Strickler, et al. (1990). "Two-photon laser scanning fluorescence microscopy." Science **248**(4951): 73-6.
- Dittgen, T., A. Nimmerjahn, et al. (2004). "Lentivirus-based genetic manipulations of cortical neurons and their optical and electrophysiological monitoring in vivo." Proc Natl Acad Sci U S A **101**(52): 18206-11.

- Dityatev, A. and M. Schachner (2003). "Extracellular matrix molecules and synaptic plasticity." Nat Rev Neurosci **4**(6): 456-68.
- Dong, H., Z. Shao, et al. (2004). "Differential depression of inhibitory synaptic responses in feedforward and feedback circuits between different areas of mouse visual cortex." J Comp Neurol **475**(3): 361-73.
- Dong, H., Q. Wang, et al. (2004). "Experience-dependent development of feedforward and feedback circuits between lower and higher areas of mouse visual cortex." Vision Res **44**(28): 3389-400.
- Douglas, R. J. and K. A. Martin (2004). "Neuronal circuits of the neocortex." Annu Rev Neurosci **27**: 419-51.
- Drager, U. C. (1978). "Observations on monocular deprivation in mice." J Neurophysiol **41**(1): 28-42.
- Drobizhev, M., S. Tillo, et al. (2009). "Absolute two-photon absorption spectra and two-photon brightness of orange and red fluorescent proteins." J Phys Chem B **113**(4): 855-9.
- Ducros, M., L. Moreaux, et al. (2009). "Spectral unmixing: analysis of performance in the olfactory bulb in vivo." PLoS One **4**(2): e4418.
- Fagiolini, M. and T. K. Hensch (2000). "Inhibitory threshold for critical-period activation in primary visual cortex." Nature **404**(6774): 183-6.
- Feldman, D. E. (2009). "Synaptic mechanisms for plasticity in neocortex." Annu Rev Neurosci **32**: 33-55.
- Feng, G., R. H. Mellor, et al. (2000). "Imaging neuronal subsets in transgenic mice expressing multiple spectral variants of GFP." Neuron **28**(1): 41-51.
- Fernandez, F., W. Morishita, et al. (2007). "Pharmacotherapy for cognitive impairment in a mouse model of Down syndrome." Nat Neurosci **10**(4): 411-3.
- Fischer, Q. S., A. Graves, et al. (2007). "Monocular deprivation in adult mice alters visual acuity and single-unit activity." Learn Mem **14**(4): 277-86.
- Florence, S. L., H. B. Taub, et al. (1998). "Large-scale sprouting of cortical connections after peripheral injury in adult macaque monkeys." Science **282**(5391): 1117-21.
- Frenkel, M. Y. and M. F. Bear (2004). "How monocular deprivation shifts ocular dominance in visual cortex of young mice." Neuron **44**(6): 917-23.

- Frenkel, M. Y., N. B. Sawtell, et al. (2006). "Instructive effect of visual experience in mouse visual cortex." Neuron **51**(3): 339-49.
- Froemke, R. C., M. M. Merzenich, et al. (2007). "A synaptic memory trace for cortical receptive field plasticity." Nature **450**(7168): 425-9.
- Fuhrmann, J. C., S. Kins, et al. (2002). "Gephyrin interacts with Dynein light chains 1 and 2, components of motor protein complexes." J Neurosci **22**(13): 5393-402.
- Gandhi, S. P., Y. Yanagawa, et al. (2008). "Delayed plasticity of inhibitory neurons in developing visual cortex." Proc Natl Acad Sci U S A **105**(43): 16797-802.
- Gascon, S., J. A. Paez-Gomez, et al. (2008). "Dual-promoter lentiviral vectors for constitutive and regulated gene expression in neurons." J Neurosci Methods **168**(1): 104-12.
- Gilbert, C. D. (1998). "Adult cortical dynamics." Physiol Rev **78**(2): 467-85.
- Goel, A. and H. K. Lee (2007). "Persistence of experience-induced homeostatic synaptic plasticity through adulthood in superficial layers of mouse visual cortex." J Neurosci **27**(25): 6692-700.
- Gonchar, Y. and A. Burkhalter (2003). "Distinct GABAergic targets of feedforward and feedback connections between lower and higher areas of rat visual cortex." J Neurosci **23**(34): 10904-12.
- Göppert-Mayer, M. (1931). "Über Elementarakte mit zwei Quantensprüngen." Annalen der Physik **401**(3): 273-294.
- Gordon, J. A. and M. P. Stryker (1996). "Experience-dependent plasticity of binocular responses in the primary visual cortex of the mouse." J Neurosci **16**(10): 3274-86.
- Gray, N. W., R. M. Weimer, et al. (2006). "Rapid redistribution of synaptic PSD-95 in the neocortex in vivo." PLoS Biol **4**(11): e370.
- Grutzendler, J., N. Kasthuri, et al. (2002). "Long-term dendritic spine stability in the adult cortex." Nature **420**(6917): 812-6.
- Hanover, J. L., Z. J. Huang, et al. (1999). "Brain-derived neurotrophic factor overexpression induces precocious critical period in mouse visual cortex." J Neurosci **19**(22): RC40.
- Harauzov, A., M. Spolidoro, et al. (2010). "Reducing intracortical inhibition in the adult visual cortex promotes ocular dominance plasticity." J Neurosci **30**(1): 361-71.

- Hartig, W., A. Derouiche, et al. (1999). "Cortical neurons immunoreactive for the potassium channel Kv3.1b subunit are predominantly surrounded by perineuronal nets presumed as a buffering system for cations." Brain Res **842**(1): 15-29.
- Haruta, M. and Y. Hata (2007). "Experience-driven axon retraction without binocular imbalance in developing visual cortex." Curr Biol **17**(1): 37-42.
- Hata, Y. and M. P. Stryker (1994). "Control of thalamocortical afferent rearrangement by postsynaptic activity in developing visual cortex." Science **265**(5179): 1732-5.
- Hata, Y., T. Tsumoto, et al. (1999). "Selective pruning of more active afferents when cat visual cortex is pharmacologically inhibited." Neuron **22**(2): 375-81.
- He, H. Y., W. Hodos, et al. (2006). "Visual deprivation reactivates rapid ocular dominance plasticity in adult visual cortex." J Neurosci **26**(11): 2951-5.
- Helmchen, F. and W. Denk (2005). "Deep tissue two-photon microscopy." Nat Methods **2**(12): 932-40.
- Hendry, S. H., J. Fuchs, et al. (1990). "Distribution and plasticity of immunocytochemically localized GABAA receptors in adult monkey visual cortex." J Neurosci **10**(7): 2438-50.
- Hendry, S. H., M. M. Huntsman, et al. (1994). "GABAA receptor subunit immunoreactivity in primate visual cortex: distribution in macaques and humans and regulation by visual input in adulthood." J Neurosci **14**(4): 2383-401.
- Hendry, S. H. and E. G. Jones (1986). "Reduction in number of immunostained GABAergic neurones in deprived-eye dominance columns of monkey area 17." Nature **320**(6064): 750-3.
- Hendry, S. H. and E. G. Jones (1988). "Activity-dependent regulation of GABA expression in the visual cortex of adult monkeys." Neuron **1**(8): 701-12.
- Hensch, T. K. (2005). "Critical period plasticity in local cortical circuits." Nat Rev Neurosci **6**(11): 877-88.
- Hensch, T. K., M. Fagiolini, et al. (1998). "Local GABA circuit control of experience-dependent plasticity in developing visual cortex." Science **282**(5393): 1504-8.
- Hersch, S. M. and E. L. White (1981). "Quantification of synapses formed with apical dendrites of Golgi-impregnated pyramidal cells: variability in thalamocortical

- inputs, but consistency in the ratios of asymmetrical to symmetrical synapses." Neuroscience **6**(6): 1043-51.
- Hirsch, J. A. and C. D. Gilbert (1993). "Long-term changes in synaptic strength along specific intrinsic pathways in the cat visual cortex." J Physiol **461**: 247-62.
- Hofer, S. B., T. D. Mrsic-Flogel, et al. (2006). "Prior experience enhances plasticity in adult visual cortex." Nat Neurosci **9**(1): 127-32.
- Hofer, S. B., T. D. Mrsic-Flogel, et al. (2009). "Experience leaves a lasting structural trace in cortical circuits." Nature **457**(7227): 313-7.
- Holmgren, C., T. Harkany, et al. (2003). "Pyramidal cell communication within local networks in layer 2/3 of rat neocortex." J Physiol **551**(Pt 1): 139-53.
- Holtmaat, A. and K. Svoboda (2009). "Experience-dependent structural synaptic plasticity in the mammalian brain." Nat Rev Neurosci **10**(9): 647-58.
- Holtmaat, A., L. Wilbrecht, et al. (2006). "Experience-dependent and cell-type-specific spine growth in the neocortex." Nature **441**(7096): 979-83.
- Holtmaat, A. J., J. T. Trachtenberg, et al. (2005). "Transient and persistent dendritic spines in the neocortex in vivo." Neuron **45**(2): 279-91.
- Huang, Z. J., A. Kirkwood, et al. (1999). "BDNF regulates the maturation of inhibition and the critical period of plasticity in mouse visual cortex." Cell **98**(6): 739-55.
- Hubel, D. H. and T. N. Wiesel (1970). "The period of susceptibility to the physiological effects of unilateral eye closure in kittens." J Physiol **206**(2): 419-36.
- Hubel, D. H., T. N. Wiesel, et al. (1977). "Plasticity of ocular dominance columns in monkey striate cortex." Philos Trans R Soc Lond B Biol Sci **278**(961): 377-409.
- Jones, E. G. and T. P. Powell (1969). "Morphological variations in the dendritic spines of the neocortex." J Cell Sci **5**(2): 509-29.
- Kaiser, K. M., J. Lubke, et al. (2004). "Postsynaptic calcium influx at single synaptic contacts between pyramidal neurons and bitufted interneurons in layer 2/3 of rat neocortex is enhanced by backpropagating action potentials." J Neurosci **24**(6): 1319-29.
- Kalatsky, V. A. and M. P. Stryker (2003). "New paradigm for optical imaging: temporally encoded maps of intrinsic signal." Neuron **38**(4): 529-45.

- Kameyama, K., K. Sohya, et al. (2010). "Differences in binocularity and ocular dominance plasticity between GABAergic and excitatory cortical neurons." J Neurosci **30**(4): 1551-1559.
- Katz, L. C. and C. J. Shatz (1996). "Synaptic activity and the construction of cortical circuits." Science **274**(5290): 1133-8.
- Kawano, H., T. Kogure, et al. (2008). "Two-photon dual-color imaging using fluorescent proteins." Nat Methods **5**(5): 373-4.
- Keck, T., T. D. Mrsic-Flogel, et al. (2008). "Massive restructuring of neuronal circuits during functional reorganization of adult visual cortex." Nat Neurosci **11**(10): 1162-7.
- Kelsch, W., C. W. Lin, et al. (2008). "Sequential development of synapses in dendritic domains during adult neurogenesis." Proc Natl Acad Sci U S A **105**(43): 16803-8.
- Kirkwood, A. and M. F. Bear (1994). "Hebbian synapses in visual cortex." J Neurosci **14**(3 Pt 2): 1634-45.
- Kleschevnikov, A. M., P. V. Belichenko, et al. (2004). "Hippocampal long-term potentiation suppressed by increased inhibition in the Ts65Dn mouse, a genetic model of Down syndrome." J Neurosci **24**(37): 8153-60.
- Knott, G. W., A. Holtmaat, et al. (2006). "Spine growth precedes synapse formation in the adult neocortex in vivo." Nat Neurosci **9**(9): 1117-24.
- Knudsen, E. I. (2002). "Instructed learning in the auditory localization pathway of the barn owl." Nature **417**(6886): 322-8.
- Kogure, T., S. Karasawa, et al. (2006). "A fluorescent variant of a protein from the stony coral *Montipora* facilitates dual-color single-laser fluorescence cross-correlation spectroscopy." Nat Biotechnol **24**(5): 577-81.
- Kubota, Y., G. Karube, et al. (2007). "Dendritic dimensions of cortical nonpyramidal cells." Society for Neuroscience Abstracts.
- Lee, W. C., J. L. Chen, et al. (2008). "A dynamic zone defines interneuron remodeling in the adult neocortex." Proc Natl Acad Sci U S A **105**(50): 19968-73.
- Lee, W. C., H. Huang, et al. (2006). "Dynamic remodeling of dendritic arbors in GABAergic interneurons of adult visual cortex." PLoS Biol **4**(2): e29.

- LeVay, S., T. N. Wiesel, et al. (1980). "The development of ocular dominance columns in normal and visually deprived monkeys." J Comp Neurol **191**(1): 1-51.
- Linden, M. L., A. J. Heynen, et al. (2009). "Thalamic activity that drives visual cortical plasticity." Nat Neurosci **12**(4): 390-2.
- Linkenhoker, B. A., C. G. von der Ohe, et al. (2005). "Anatomical traces of juvenile learning in the auditory system of adult barn owls." Nat Neurosci **8**(1): 93-8.
- Livet, J., T. A. Weissman, et al. (2007). "Transgenic strategies for combinatorial expression of fluorescent proteins in the nervous system." Nature **450**(7166): 56-62.
- Lois, C., E. J. Hong, et al. (2002). "Germline transmission and tissue-specific expression of transgenes delivered by lentiviral vectors." Science **295**(5556): 868-72.
- Maas, C., N. Tagnaouti, et al. (2006). "Neuronal cotransport of glycine receptor and the scaffold protein gephyrin." J Cell Biol **172**(3): 441-51.
- Madisen, L., T. A. Zwingman, et al. (2009). "A robust and high-throughput Cre reporting and characterization system for the whole mouse brain." Nat Neurosci **13**(1): 133-40.
- Maffei, A. and G. G. Turrigiano (2008). "Multiple modes of network homeostasis in visual cortical layer 2/3." J Neurosci **28**(17): 4377-84.
- Majewska, A. K., J. R. Newton, et al. (2006). "Remodeling of synaptic structure in sensory cortical areas in vivo." J Neurosci **26**(11): 3021-9.
- Markram, H., M. Toledo-Rodriguez, et al. (2004). "Interneurons of the neocortical inhibitory system." Nat Rev Neurosci **5**(10): 793-807.
- Mataga, N., Y. Mizuguchi, et al. (2004). "Experience-dependent pruning of dendritic spines in visual cortex by tissue plasminogen activator." Neuron **44**(6): 1031-41.
- Matter, C., M. Pribadi, et al. (2009). "Delta-catenin is required for the maintenance of neural structure and function in mature cortex in vivo." Neuron **64**(3): 320-7.
- Maunsell, J. H. and D. C. van Essen (1983). "The connections of the middle temporal visual area (MT) and their relationship to a cortical hierarchy in the macaque monkey." J Neurosci **3**(12): 2563-86.
- Maya Vetencourt, J. F., A. Sale, et al. (2008). "The antidepressant fluoxetine restores plasticity in the adult visual cortex." Science **320**(5874): 385-8.

- McBain, C. J. and A. Fisahn (2001). "Interneurons unbound." Nat Rev Neurosci **2**(1): 11-23.
- Nagai, T., K. Ibata, et al. (2002). "A variant of yellow fluorescent protein with fast and efficient maturation for cell-biological applications." Nat Biotechnol **20**(1): 87-90.
- Nassi, J. J. and E. M. Callaway (2009). "Parallel processing strategies of the primate visual system." Nat Rev Neurosci **10**(5): 360-72.
- Niell, C. M., M. P. Meyer, et al. (2004). "In vivo imaging of synapse formation on a growing dendritic arbor." Nat Neurosci **7**(3): 254-60.
- Oray, S., A. Majewska, et al. (2004). "Dendritic spine dynamics are regulated by monocular deprivation and extracellular matrix degradation." Neuron **44**(6): 1021-30.
- Peters, A. (2002). "Examining neocortical circuits: some background and facts." J Neurocytol **31**(3-5): 183-93.
- Pizzorusso, T., P. Medini, et al. (2002). "Reactivation of ocular dominance plasticity in the adult visual cortex." Science **298**(5596): 1248-51.
- Pizzorusso, T., P. Medini, et al. (2006). "Structural and functional recovery from early monocular deprivation in adult rats." Proc Natl Acad Sci U S A **103**(22): 8517-22.
- Prusky, G. T., N. M. Alam, et al. (2006). "Enhancement of vision by monocular deprivation in adult mice." J Neurosci **26**(45): 11554-61.
- Rahim, A. A., A. M. Wong, et al. (2009). "Efficient gene delivery to the adult and fetal CNS using pseudotyped non-integrating lentiviral vectors." Gene Ther **16**(4): 509-20.
- Ramón y Cajal, S. (1911). Histologie du Systeme Nerveux de l'Homme et des Vertebres Paris, Maloine.
- Rockland, K. S. and D. N. Pandya (1979). "Laminar origins and terminations of cortical connections of the occipital lobe in the rhesus monkey." Brain Res **179**(1): 3-20.
- Rubenstein, J. L. and M. M. Merzenich (2003). "Model of autism: increased ratio of excitation/inhibition in key neural systems." Genes Brain Behav **2**(5): 255-67.
- Ruthazer, E. S., J. Li, et al. (2006). "Stabilization of axon branch dynamics by synaptic maturation." J Neurosci **26**(13): 3594-603.

- Saghatelyan, A. K., A. Dityatev, et al. (2001). "Reduced perisomatic inhibition, increased excitatory transmission, and impaired long-term potentiation in mice deficient for the extracellular matrix glycoprotein tenascin-R." Mol Cell Neurosci **17**(1): 226-40.
- Sale, A., J. F. Maya Vetencourt, et al. (2007). "Environmental enrichment in adulthood promotes amblyopia recovery through a reduction of intracortical inhibition." Nat Neurosci **10**(6): 679-81.
- Sato, M. and M. P. Stryker (2008). "Distinctive features of adult ocular dominance plasticity." J Neurosci **28**(41): 10278-86.
- Sawtell, N. B., M. Y. Frenkel, et al. (2003). "NMDA receptor-dependent ocular dominance plasticity in adult visual cortex." Neuron **38**(6): 977-85.
- Schluter, O. M., W. Xu, et al. (2006). "Alternative N-terminal domains of PSD-95 and SAP97 govern activity-dependent regulation of synaptic AMPA receptor function." Neuron **51**(1): 99-111.
- Schmitt, B., P. Knaus, et al. (1987). "The Mr 93,000 polypeptide of the postsynaptic glycine receptor complex is a peripheral membrane protein." Biochemistry **26**(3): 805-11.
- Semple-Rowland, S. L., K. S. Eccles, et al. (2007). "Targeted expression of two proteins in neural retina using self-inactivating, insulated lentiviral vectors carrying two internal independent promoters." Mol Vis **13**: 2001-11.
- Shaner, N. C., R. E. Campbell, et al. (2004). "Improved monomeric red, orange and yellow fluorescent proteins derived from *Discosoma* sp. red fluorescent protein." Nat Biotechnol **22**(12): 1567-72.
- Shaner, N. C., P. A. Steinbach, et al. (2005). "A guide to choosing fluorescent proteins." Nat Methods **2**(12): 905-9.
- Shatz, C. J. and M. P. Stryker (1978). "Ocular dominance in layer IV of the cat's visual cortex and the effects of monocular deprivation." J Physiol **281**: 267-83.
- Singer, W. (1996). "Neurophysiology: the changing face of inhibition." Curr Biol **6**(4): 395-7.
- Smith, G. B., A. J. Heynen, et al. (2009). "Bidirectional synaptic mechanisms of ocular dominance plasticity in visual cortex." Philos Trans R Soc Lond B Biol Sci **364**(1515): 357-67.

- Somogyi, P., G. Tamas, et al. (1998). "Salient features of synaptic organisation in the cerebral cortex." Brain Res Brain Res Rev **26**(2-3): 113-35.
- Stepanyants, A., P. R. Hof, et al. (2002). "Geometry and structural plasticity of synaptic connectivity." Neuron **34**(2): 275-88.
- Stettler, D. D., H. Yamahachi, et al. (2006). "Axons and synaptic boutons are highly dynamic in adult visual cortex." Neuron **49**(6): 877-87.
- Stott, S. R. and D. Kirik (2006). "Targeted in utero delivery of a retroviral vector for gene transfer in the rodent brain." Eur J Neurosci **24**(7): 1897-906.
- Tabata, H. and K. Nakajima (2001). "Efficient in utero gene transfer system to the developing mouse brain using electroporation: visualization of neuronal migration in the developing cortex." Neuroscience **103**(4): 865-72.
- Tillo, S. E., T. E. Hughes, et al. (2010). "A new approach to dual-color two-photon microscopy with fluorescent proteins." BMC Biotechnol **10**: 6.
- Trachtenberg, J. T., B. E. Chen, et al. (2002). "Long-term in vivo imaging of experience-dependent synaptic plasticity in adult cortex." Nature **420**(6917): 788-94.
- Triller, A., F. Cluzaud, et al. (1985). "Distribution of glycine receptors at central synapses: an immunoelectron microscopy study." J Cell Biol **101**(2): 683-8.
- Turrigiano, G. G. (2008). "The self-tuning neuron: synaptic scaling of excitatory synapses." Cell **135**(3): 422-35.
- Turrigiano, G. G. and S. B. Nelson (2004). "Homeostatic plasticity in the developing nervous system." Nat Rev Neurosci **5**(2): 97-107.
- Walsh, C. and C. L. Cepko (1992). "Widespread dispersion of neuronal clones across functional regions of the cerebral cortex." Science **255**(5043): 434-40.
- White, E. L. and M. P. Rock (1980). "Three-dimensional aspects and synaptic relationships of a Golgi-impregnated spiny stellate cell reconstructed from serial thin sections." J Neurocytol **9**(5): 615-36.
- White, E. L., E. Weinfeld, et al. (2004). "Quantitative analysis of synaptic distribution along thalamocortical axons in adult mouse barrels." J Comp Neurol **479**(1): 56-69.
- Wiesel, T. N. and D. H. Hubel (1963). "Single-Cell Responses in Striate Cortex of Kittens Deprived of Vision in One Eye." J Neurophysiol **26**: 1003-17.

- Wiesel, T. N. and D. H. Hubel (1965). "Comparison of the effects of unilateral and bilateral eye closure on cortical unit responses in kittens." J Neurophysiol **28**(6): 1029-40.
- Xu, T., X. Yu, et al. (2009). "Rapid formation and selective stabilization of synapses for enduring motor memories." Nature **462**(7275): 915-9.
- Yamahachi, H., S. A. Marik, et al. (2009). "Rapid axonal sprouting and pruning accompany functional reorganization in primary visual cortex." Neuron **64**(5): 719-29.
- Yamashita, A., K. Valkova, et al. (2003). "Rearrangement of synaptic connections with inhibitory neurons in developing mouse visual cortex." J Comp Neurol **464**(4): 426-37.
- Yang, G., F. Pan, et al. (2009). "Stably maintained dendritic spines are associated with lifelong memories." Nature **462**(7275): 920-4.
- Yazaki-Sugiyama, Y., S. Kang, et al. (2009). "Bidirectional plasticity in fast-spiking GABA circuits by visual experience." Nature **462**(7270): 218-21.
- Young, P., L. Qiu, et al. (2008). "Single-neuron labeling with inducible Cre-mediated knockout in transgenic mice." Nat Neurosci **11**(6): 721-8.
- Zimmermann, T. (2005). "Spectral imaging and linear unmixing in light microscopy." Adv Biochem Eng Biotechnol **95**: 245-65.
- Zipfel, W. R., R. M. Williams, et al. (2003). "Nonlinear magic: multiphoton microscopy in the biosciences." Nat Biotechnol **21**(11): 1369-77.